Geo-information Science and Remote Sensing

Space for time - How do peatland vegetation patterns develop through time?

Timon Weitkamp

March 2018

WAGENINGEN
UNIVERSITY & RESEARCH

Space for time - How do peatland vegetation patterns develop through time?

Timon Weitkamp

Registration number 930202937040

<u>Supervisors:</u>

dr.ir. Lammert Kooistra
dr. Jelmer Nijp

A thesis submitted in partial fulfilment of the degree of Master of Science
at Wageningen University and Research Centre,
The Netherlands.

March 2018
Wageningen, The Netherlands

Abstract

Boreal peatlands grow slow, thus tracking the spatial vegetation pattern development within a peatland requires a long time. One way of analysing pattern development, without taking the expected long time, is by using a chronosequence. This method can be used in an area where land emerges due to glacial rebound and new peatlands develop, such as northern Sweden. These peatland patterns are made up of densely vegetated ridges (hummock), interspersed with sparsely vegetated pools (hollows). This research used high-resolution aerial imagery to classify peatlands in five land cover classes, after which the classified hummock patches were used to analyse pattern development. The age of peatlands was based on the elevation and isostatic rebound, so when the peatland was located on the shoreline. The patterns were quantified with pattern metrics and correlated with terrain characteristics in generalised additive models (GAMs). Overall, this research found that hummock patches start small in young peatlands, and grow together to form long, broad patches as the peatland ages (taking at least 2000 years), however, this does not occur in all peatlands. The minor & major range and the radius of gyration (the mean distance between each cell in a patch and a patch centroid) had the highest correlations with age (r^2 = 0.263, 0.214 and 0.128, respectively). The total catchment area above a peatland had the highest correlation of the terrain characteristics (r^2 = 0.397). Factors that contributed to the low R-squared are the location and the number of sampling points. In conclusion, it is possible to analyse spatial vegetation pattern development by using high-resolution aerial imagery and pattern metrics.

Keywords: peatland, pattern, hummock, hollow, terrain, metric, Generalized Additive Model (GAM), aerial imagery

Acknowledgements

Contents

List of Figures

List of Tables

1 | Introduction

1.1 Context and background

Peatlands are ecosystems with higher net primary production than organic matter decomposition rate on the long term, leading to the accumulation of a deposit full of incomplete decomposed organic matter (Wieder, Vitt, & Benscoter, 2006). Peatlands develop due to four processes, the most prevailing being the paludification (or waterlogging) of drier areas, due to water table rise or changing climate conditions. The second process is the gradually filling up of water bodies. The last two are related to glaciation, with peat forming on freshly uncovered soils due to glacial retreat or isostatic rebound being the third process, and peat formation on former lake basins being the fourth (Wieder & Vitt, 2006).

Even though peat layers develop gradually, peatlands form a significant global terrestrial pool of organic matter and carbon (Tuittila et al., 2013). Northern peatlands cover just 2 to 3% of the earth's surface. However, nearly a third of the world's terrestrial soil carbon is stored in these peatlands (Eppinga, Rietkerk, Wassen, & De Ruiter, 2009; Gorham, 1991; Wieder & Vitt, 2006), meaning their ecological and societal importance is much bigger than expected for such small surface. These peatlands are also located in areas that are expected to have the highest increase in precipitation and temperature in the next decades (Houghton, Meira Filho, & Callender, 1995).

Northern peatlands can be divided into fens and bogs, depending on their hydrology and vegetation (Tuittila et al., 2013), with fens being influenced by groundwater and bogs only by precipitation (Vitt, Bayley, & Jin, 1995). A succession from fen to bog occurs when the surface of the peatland rises above the surrounding surface to the point that there is no influence of groundwater anymore. The peat accumulation increases the distance between the peat surface and the groundwater, and compact deeper laying peat material, which decreases the permeability. At this point, the vegetation depends on precipitation for water and nutrients (ombrotrophic), as the rooting zone becomes more isolated from the mineral-rich groundwater and soil (Kuhry & Turunen, 2006).

Peatland ecosystems often show spatial vegetation patterns, such as regular string patterns (Figure 1.1 top) of densely vegetated ridges (*hummocks*), perpendicular to the slope, which are interspersed with sparse vegetated pools (*hollows*). Another example is a maze-like pattern (Figure 1.1 bottom), which is a matrix of hummocks and hollows without a specific orientation, unlike string patterns (Rietkerk, Dekker, de Ruiter, & van de Koppel, 2004). The spatial structure of these patterns is defined as patchiness.

Figure 1.1: *Hummock-hollow patterns on a slope (top), also called string patters, and on a flatter area (bottom), also called maze-like patterns*

The patterning itself can be explained by a positive feedback between plant productivity and groundwater depth on elevated, drier sites, mainly due to increased production of vascular plants (Rietkerk, Dekker, de Ruiter, & van de Koppel, 2004). The positive feedback is maintained because the vascular plants on hummocks attract nutrient flows in the water, due to differences in the transpiration rate (Rietkerk, Dekker, Wassen, Verkroost, & Bierkens, 2004). Although models suggest that small random hummocks will grow together as a peatland grows older, due to the positive feedbacks ((Eppinga, De Ruiter, Wassen, & Rietkerk, 2009; Eppinga, Rietkerk, et al., 2009; Rietkerk, Dekker, de Ruiter, & van de Koppel, 2004), there is insufficient empirical data on how these patterns form.

As northern peatlands are located in areas that are expected to have the greatest increase in precipitation and temperature in the next decades, internal peatland dynamics may be affected in such a way that peatlands may switch from sinks to sources of atmospheric carbon (Bridgham, Johnston, Pastor, & Updegraff, 1995; Yu, Campbell, Vitt, & Apps, 2001). However, peatlands

are quite resilient to changes in climatic conditions (Belyea & Clymo, 2001). Nevertheless, this resilience is lost when environmental thresholds are passed due to changes in climate, which in turn may cause a shift to another stable state, with different surface patterns (Belyea & Malmer, 2004; Eppinga, Rietkerk, et al., 2009). This transition also results in different rates of carbon decomposition and sequestration; however, these systems are not fully understood yet (Belyea & Malmer, 2004). This transition is called a catastrophic shift, when an ecosystem shifts to an alternate stable state, which is not quickly reversed or cannot be reversed at all (Kéfi et al., 2014; Rietkerk, Dekker, de Ruiter, & van de Koppel, 2004).

This catastrophic shift in relation to spatial vegetation patterns has been analysed already. Scheffer et al. (2009) modelled desert vegetation pattern development and showed that they become more regular when a catastrophic shift to a barren state is approaching. If these patterns change predictably, they may be used as an early-warning signal for a nearing catastrophic shift. This raises the question whether peatland vegetation patterns could also be used as an early-warning signal for a catastrophic shift.

1.2 Problem description

As previously mentioned, there is a need to understand the internal dynamics in peatlands with changing environmental conditions, observable through spatial vegetation patterns (i.e. hummocks and hollows).

One way of understanding the dynamics of pattern development is by taking core samples of the peat, up to depths of 2.5 meters (De Vleeschouwer, Chambers, & Swindles, 2010). However, doing this for a whole patch of peatland is both time-consuming and very destructive, as many cores are needed. Also, the spatial pattern is destroyed and not suitable for reconstruction. Instead, different aged peatlands along a spatial chronosequence (a sequence of peatlands that differ in their profile due to differences in their age, also referred to as a Spac-for-Time approach) can be analysed, and as such a larger spatial extent can be examined in a non-destructive way, at the same time. The chronosequence allows comparison of the links between vegetation and the environment (Clarkson, Schipper, & Lehmann, 2004). Aerial imagery of these differently aged peatlands can then be used to understand temporal processes. In an area where new land emerges due to isostatic rebound, such as Sweden and Finland, this method can be used to understand the dynamics of vegetation patterning (Tuittila et al., 2013). As mentioned earlier, one of the processes of peatland formation is because of land becoming available due to glacial retreat.

In Canada, a study has been done by Klinger and Short (1996), which studied bog successions in a chronosequence, in an area with isostatic uplift. The isostatic uplift causes new land to emerge and changes

the base level, topography and drainage network. Surface hydrology, and to a lesser extent the climate, were the main factors controlling the development of the lowlands. In the same peat basin, Glaser, Siegel, Reeve, Janssens, and Janecky (2004) found that peatland succession seemed to be driven by the tectonic forces, rather than climate.

But analysing the patterns is not the only challenge. Local nutrient concentrations and hydrology behaviour can also differ from location to location. Hence, when comparing vegetation patterns, these factors need to be considered.

Although vegetation patterns can be compared, being able to quantify these patterns in a way that is reproducible and accurate is challenging. In part, this is because of the use of open data, which can have their limitations such as different spatial resolutions and data collection moments. Quantification of these spatial patterns can be done with statistics, for example with patch density, size and shape metrics (McGarigal, Cushman, Neel, & Ene, 2002). Other statistics are mentioned in Kéfi et al. (2014), such as spatial variance, and the Fast Fourier Transform (FFT) (Arrell, Wise, Wood, & Donoghue, 2008).

1.3 Research objective & questions

Peatland vegetation patterns develop through time; however, it is not fully understood yet what the link is between vegetation and the environment. Therefore, the main research objective is to try to understand vegetation pattern development of northern peatlands through time, using high-resolution images for a spatial chronosequence of peatlands.

The hypothesis is that vegetation pattern metrics can be used to estimate the development of the peatland, assuming spatial patterns predictably develop over time. Based on the objectives and the hypothesis the research questions are:

1. Can aerial images be used to detect spatial vegetation patterns in peatlands?

2. Do vegetation patterns change when the peatland grows older?

3. Which vegetation pattern descriptors or metrics best indicate such changes?

4. Which environmental characteristics influence the development of spatial vegetation patterns?

1.4 Reading guide

Chapter 2 will provide additional literature which can help with understanding the various concepts. In Chapter 3 the study area, data description and methodology are described. Chapter 4 shows the results and Chapter 5 the discussion. The last chapter, Chapter 6, concludes this thesis.

2 | Literature

2.1 Swedish peatland landscapes

The area covered by at least half a meter thick peat stock has been estimated to be around 64.000 km². This corresponds to about 15 percent of Sweden's land area (StatisticSweden, 2013). The largest peatland areas are found in northern Sweden (Figure 2.1). Figures 2.2 and 2.3 show what peatlands are look like. These images show that a peatland landscape consists of lakes, hummocks, hollows and on the drier, more elevated areas, forests. In the peatland itself, there are hardly any trees, with the few occurring trees growing on hummocks. Other vegetation includes short sedge grass, shrubs and peat mosses.

Figure 2.1: Distribution of peatlands (= Torvmarksförekomst, brown) in Sweden (Source: Rikstäckande jordartsinformation, SGU 2011).

Figure 2.2: Photos of peatlands in Västerbotten, Sweden (Source: http://www.lansstyrelsen.se/Vasterbotten/Sv/djur-och-natur/skyddad-natur).

2.2 Supervised maximum likelihood classification of peat

Different classification methods can be adopted for land cover classification from remote sensing images. Maximum likelihood assigns pixels to classes, based on their

What both studies show is that although there are other methods than MLC, which produce more homogeneous classification results, there are not always better. Poulin et al. (2002) mention confusion between three pairs of habitats, namely between shrubs and herbs, and Haapanen and Tokola (2007) mention that using fewer classes achieves better overall results, and that the number of classes depends on the definition of the end-users' need.

2.3   Landscape metrics

The identification of local anisotropy (different properties in different directions) can be done by using Fast Fourier Transforms (FFT) (Bergonnier, Hild, & Roux, 2007), which results in minor and major ranges of patches, and a measure of anisotropy. Another way to quantifies the areal extent and spatial distribution of patches is by using pattern metrics, such as with the programme FRAGSTATS McGarigal et al. (2002). These metrics are grouped by area, patch density/size, edge, shape, core area, nearest neighbour, diversity and interspersion metrics. A list of all specific metrics available can be found in Table 1 of McGarigal et al. (2002). Kéfi et al. (2014) summarises how changes in spatial vegetation patterns can provide early warning signals of approaching catastrophic shifts. The spatial indicators include quantifying spatial autocorrelation, quantifying spectral properties by Discrete Fourier Transform (DFT), spatial variance and spatial skewness, but also patch based indicators such as shapes and sizes of patches.

Figure 2.3: *Example of what a hummock and hollow look like (Photo courtesy: Mats Nilsson). Note that hummocks are slightly raised, as compared to hollows.*

spectral properties, and requires homogeneous training regions (Haapanen & Tokola, 2007). In their study, Haapanen and Tokola (2007) compared peatland classification based on maximum likelihood (MLC) and a method that uses spatial continuity in addition to spectral properties (sequential maximum a posteriori, SMAP), and found that MLC performed slightly better on fragmented areas, although SMAP produces unspeckled areas. Another comparison between classification techniques was made by Poulin, Careau, Rochefort, and Desrochers (2002), which compared MLC and a weighted MLC (WMLC). The WMLC takes into account the spatial autocorrelation among neighbouring pixels. The study found that both methods had approximately the same accuracy levels for the overall area. There were differences in common habitats (better classified by WMLC) and rare habitats, which were better classified by MLC, due to WMLC producing more homogenous classification maps. Both studies classified peatlands with a relatively coarse spatial resolution: 25x25 and 30x30 meters, respectively. Haapanen and Tokola (2007) used six classes including forest, forested peatland and treeless peatland related classes, while Poulin et al. (2002) used 13 classes, mostly herbs, shrubs and forest-related classes.

3 | Materials and methods

This chapter contains a brief introduction to the study area, a description of the used datasets and the processing steps used in this research.

3.1 Study area

To establish a chronosequence, an area of isostatic rebound is required, which is the case for the Gulf of Bothnia, the sea between Sweden and Finland. Due to the availability of field measurements on peatlands, the chosen study area is in the north-eastern province of Västerbotten in Sweden, located north/north-east of the city Umeå (63° 49′ 42.31" N, 20° 15′ 34.99" E). This area receives an annual average precipitation of 600 mm and has an average temperature of 2.6 ° C (Cimatedata.eu, n.d.). The specific study area is a transect from the coastland inwards and covers an area of 30.609 ha (Figure 3.1). The land cover in this area mainly consists of forest (23.795 ha) interspersed with many small to large lakes (983 ha) and peatlands (5.214 ha), with an occasional village (10 ha), agricultural lands (278 ha) and open fields (326 ha, Table 3.1). The transect rises from sea level to +260 m.a.s.l. nearly 40 km land inwards and varies from 5-20 km in width.

Table 3.1: *Landcover types within transect, with their area and percentage of total area.*

Land cover	Area (ha)	Percent of total
Forest	23795	78.5
Peatlands	5214	17.2
Lakes, rivers	983	3.2
Agricultural lands	278	0.9
Open fields	36	0.1
Village/houses	10	0.0

3.2 Datasets

Four main types of data are used in this study, namely: 1) aerial images, which include red, green & blue (RGB) bands and one infrared (IR) band; 2) a digital elevation model (DEM); 3) vector maps such as a terrain map (Table 3.1); and 4) field data. Each input will be explained more in depth in the following paragraphs. All data sets except the field data can be characterised as open datasets available to the public and can are available on the Swedish geoportal website[1], which has links to specific websites such as the Lantmäteriet, the land surveying office. However, some data sets require additional expenses.

---

[1] https://www.geodata.se/en/
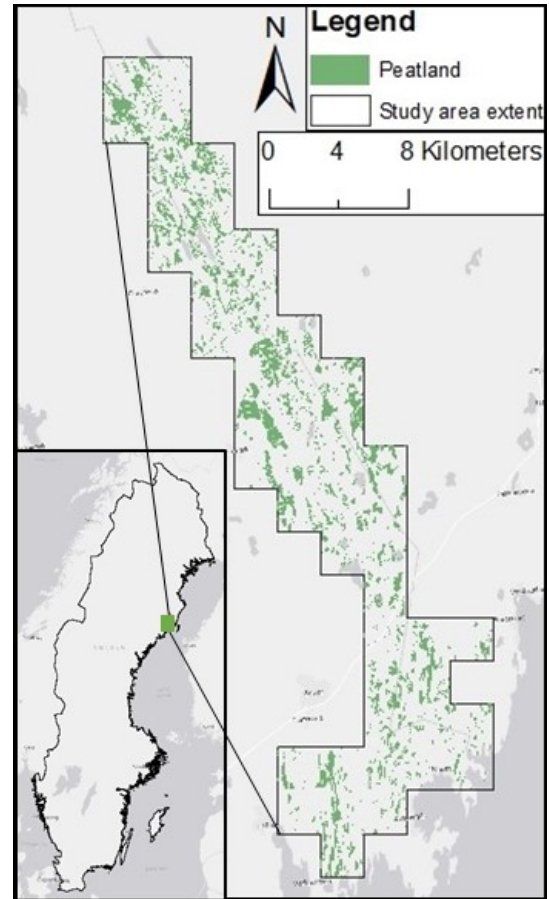
Figure 3.1: *Transect of the study area near Umeå. From the coast land inwards the transect is 40 km long. All peatlands in the area are shown, based on landcover maps from Lantäteriet (2018).*

Administrative boundaries

This dataset includes the country, province and municipality boundaries of Sweden. The administrative boundaries have remained the same since 31 December 1999, with a few adjustments throughout the years, the last one being on 1 January 2016. This dataset is used only to clip other data to only the area of interest.

Terrain map

The terrain map is used to identify peatlands, at a scale of 1: 50 000. Until 2005, information was collected through fieldwork and interpretation of aerial photographs; now there is no fieldwork anymore.

In the available terrain map, the class called ′*Annan öppen mark utan skogskontur*′ refers to open fields without forest and corresponds to peatlands. A significant part of this research is based on this data, as these peatlands are used to clip the areal images and the DEM. The location accuracy of the peatlands is 15 meters (Lantä-

Table 3.2: Input data for research, with name, type, provider, data type and acquisition date.

Name	Type	Provider	Data type (Spatial resolution)	Acquisition date
Administrative boundaries	Digitised maps	Lantmäteriet	Polygon	-
Terrain map	Digitised maps	Lantmäteriet	Polygon	-
Watershed delineation	Digitised maps	Sveriges Meteorologiska och Hydrologiska Institut (SMHI)	Polygon	-
RGB	Aerial imagery	Lantmäteriet	Raster (0.5x0.5m)	20 May/21 July 2016
IR	Aerial imagery	Lantmäteriet	Raster (0.5x0.5m)	20 May/21 July 2016
DEM	Laser scanning	Lantmäteriet	Raster (2x2m)	20 May/21 July 2016
Field data	Field measurements (location, elevation, peat depth and age)	Mats Nilsson (from SLU)	-	28 September 2008

teriet, 2018), mainly due to the difficulty in judging where the boundary between peatland and for example forest is.

Watershed delineation

This data is from the Swedish meteorology and hydrology institute (SMHI) and divides Sweden into 50.829 sub-basins. The catchments are made from manually digitised divides with map elevation curves and water objects in the background (personal comment Håkan Olsson (SMHI), 02-03-2018).

The study area spans two major watersheds, and 44 smaller watersheds (Figure 3.3), with an average area of 12 km^2, the smallest being 0.3 km^2 and the biggest being 50 km^2, with most being smaller than ten km^2 (Lantäteriet, 2018).

Aerial images (RGB, IR and DEM)

Sweden has been making regular aerial photographs of the country since the 1950s, with a few limited areas photographed since the 1930s. From 2005 onwards, acquisition of the photos happens digitally. Depending on the location (population and land use), the images are re-taken every 2 to 10 years.

The RGB, IR and DEM images within the study area have been acquired from an aeroplane on two dates, namely 20 May and 21 July of 2016. The spectral ranges of the bands are 410-610 nm (blue)), 490-680 nm (green), 590-720 nm (red) and Near IR 690-900 nm (Near IR). The resolution is 0.5 meters, and tiles of 5x5 km are available, in the Swedish coordinate system SWEREF 99 RM.

Elevation data is collected with an airborne laser scanner (LiDAR) and processed to construct a gridded terrain model, with a resolution of 2 meters. Tiles of 2.5x2.5 km are available, in the Swedish coordinate system SWEREF 99 RM.

Field measurements

Field measurements were done by Mats Nilsson, from the Swedish University of Agricultural Sciences (SLU) in Umeå, and include the location, elevation and depth of specific locations within peatlands, as well as the age (based on C14 dating).

3.3 Processing steps

The methodology for this research is divided into five main steps, which are described below (Figure 3.2). This section describes the steps of selecting suitable peatlands and aerial imagery preparation, which are eventually used for the landcover classification and the analysis of the pattern and terrain characteristics.

Step 1: Selecting suitable peatlands

In this first step, the terrain map of Sweden is used, together with a standard ArcMap satellite image base map for reference, to identify peatlands areas. Then, to select the peatlands with minimal human influence (such as drainage, logging or industry), each landcover type (in the percentage of total area) is calculated per small watershed, after which the watersheds containing industry and agriculture are excluded. Minimal human influence is desirable as patterns may be affected due to this influence. After knowing where all suitable peatlands are located, a transect can be made, and the aerial image tiles can be ordered through Lantmäteriet.
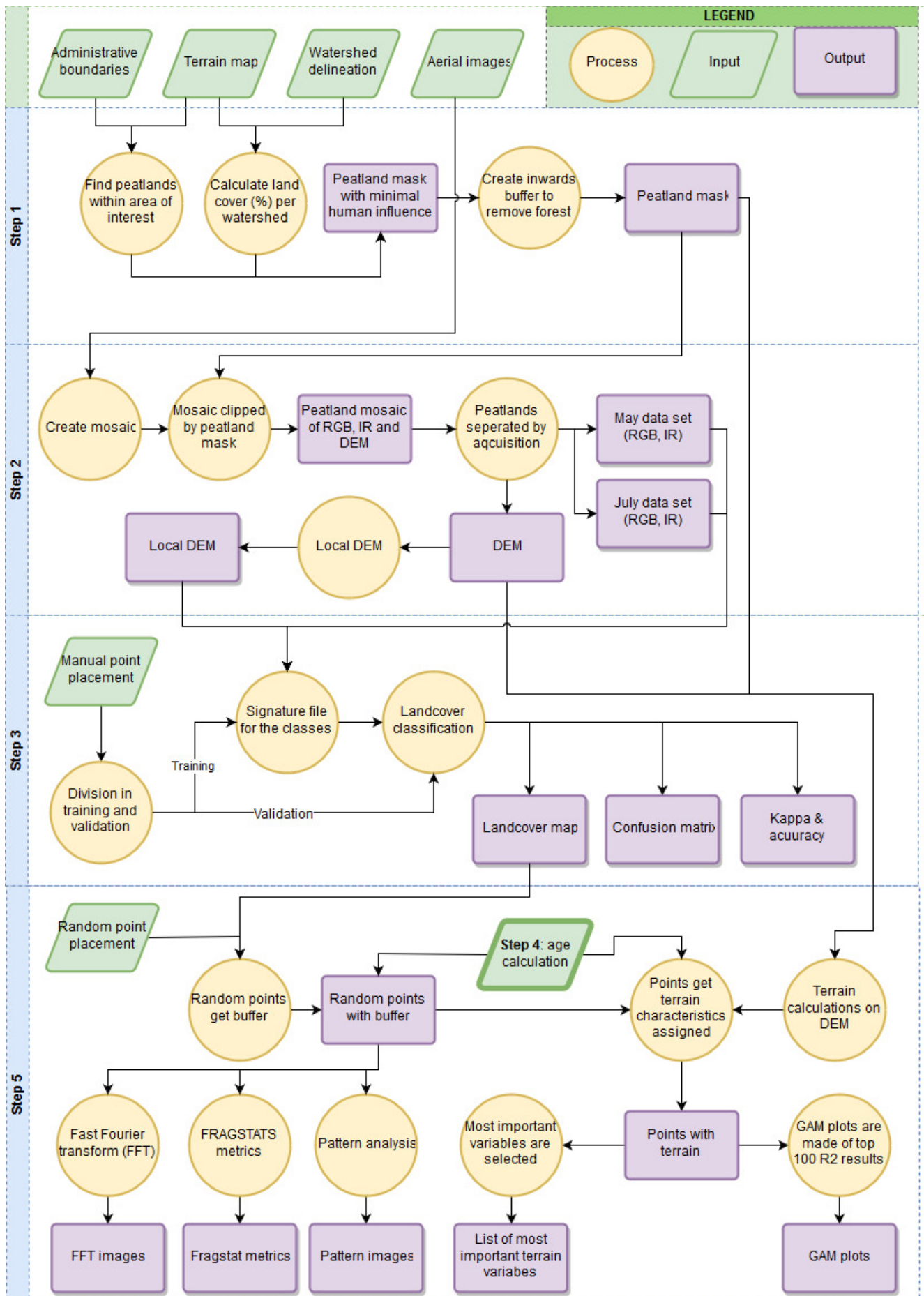
Figure 3.2: *Flowchart showing the steps of the research. Step 4 is an intermediate step, placed inside the box of step 5.*
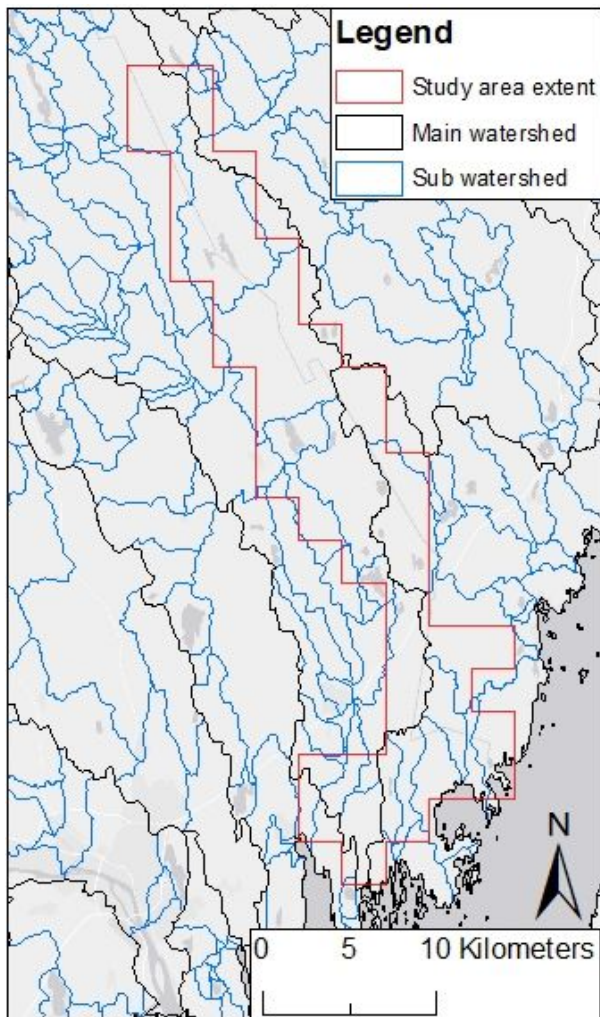
Figure 3.3: *Watershed map of the study area (red) near Umeå, with in blue the subwatersheds and black the major watersheds. The study area contains 2 major watersheds, and 44 subwatersheds.*

Next, all forests on the edges of these peatlands are removed as well, by making an inward buffer of 15 meters on the peatland polygon mask, based on the accuracy of *Annan öppen mark utan skogskontur*. This means that part of the peatland is also removed; however, due to the abundance of peatlands, the total areal loss is minimal. The advantage is that the landcover classification will be easier (see Step 3), as there is one class fewer to classify.

Step 2: Areal imagery preparation

In this step, the suitable peatlands are extracted from the total extent of the aerial imagery, which is needed for the landcover classification (Step 3).

First, mosaics are made from the separate DEM, IR and RGB images (resulting in a total of three mosaics). Next, these mosaics are clipped to the peatland polygon (Step 1). The areal images within the study area were acquired on two different dates, each with varying circumstances of weather and consequently different light intensities and reflectance's, meaning a distinction needs to be made within the mosaics, corresponding with their

acquisition date. Thus, all peatlands are divided by either of the two dates (May and July).

The DEM needs one additional step. The elevation of each cell is compared to the mean elevation of a specified neighbourhood around that cell, which results in hummocks and hollows being more visible. This local DEM is used to estimate local (micro)topography, which may aid the classification of hummocks and hollows. A similar workflow can be found in Hesse (2010) and Novák (2014) for archaeology, however, they used additional steps.

Step 3: Supervised landcover classification

Once the data was prepared, the landcover classification could start. This step describes the process of how the different areal imageries are used.

First, 104 points were distributed over the study area, per acquisition date dataset (so in total 208 points). These categories are: hummock, hollow, water, mud bottom and sedge (see Table A.1 in annex A) for the classification key). The amount of points depends on the overlap of bands that each category has with another. Water has the least overlap, while hummocks and hollows have more. Sedge and mud bottom are slightly better distinguishable (Annex A).

After randomly dividing these points into training and validation points (80% and 20%, respectively), a square buffer with 1 m radius is made around all the points, which need to contain a homogenous landcover. The training data set is used for the signature file, the validation data set is used to assess the accuracy of the classification.

The local DEM, IR and RGB from Step 2 are used to make the signature file, which is used to determine the maximum likelihood of a class for each cell. The signature is made by determining the spectral properties and local DEM within the buffer of the training points. As the training points have a predesignated landcover category, the spectral properties and local DEM will then be associated with these categories. Maximum likelihood classification assigns the pixel to classes based on their spectral properties (Anderson et al., 2010; Poulin et al., 2002).

Two signature files were made, one for each acquisition date. In the May dataset, there is still some snow, meaning an entirely different spectral signature as the July dataset. Vegetation is also at a different growing stage, in May there is more water, mud and bare soil as compared to July when vegetation grows.

The results is a landcover map, as well as a confidence map of the classification. The confidence map shows 14 levels of confidence, based on the mean vector of the signature file and the distance of the cells' value to this mean. These 14 levels are pre-determined by the maximum likelihood tool.

To assess the classification results, a confusion matrix is made, as well as Kappa's statistics (Foody, 2002) and the accuracy of the classification results, based on

Table 3.3: Dependent (pattern) and independent (terrain) variables used in analysis step. FFT = Fast Fourier Transfer

Dependent (pattern)			Independent (terrain)	
FTT	FRAGSTATS (grouped)	Spatial early warning	SAGA GIS	
Major	Area/density/edge metrics	mean	age	negative topographic openess (100 & 500m)
Minor	Shape metrics	moran	total cathment area	positive topographic openess (100 & 500m)
Aniso	Isolation/ proximity metrics	skewness	slope	slope length
Angle	Contagion/ interspersion metrics	variance	aspect	downslope gradient (0.2, 0.5, 1 & 2m)
		sdr	terrain wetness index	flowpathl

the remaining validation points. This whole step is an iterative process, mainly through adjustment of the location of training points to get better classification results. This process was stopped when the best Kappa's statistic was reached.

Step 4: Calculating peatland age based on DEM

The chronosequence makes it possible to analyse peatlands at different locations. However, location alone does not give an age. The age is needed to be able to compare pattern development. On the website of the Swedish geology institute, it is possible to go to a location and find out how high the sea level was at a certain moment in time, which results in a shoreline displacement curve. Two locations have been chosen for this research, one near the coast, and one 40 km from the coast, as the two extremes. These extremes include the highest and lowest rebound rates. An average rebound curve is made from these two, and the derived equation is used for the age calculation (Annex C). The age map ranges from 30 years near the coast to just over 10.000 years at the highest point (Figure 3.4). Berglund (2012) and Påsse and Daniels (2015) mention similar ages as the SGU data (Annex C), based on their isostatic rebound curves.

Step 5: Pattern and terrain analysis

This step uses the landcover classification map from Step 3, the original DEM from Step 2 and the peatland mask from Step 1 to quantify vegetation patterns and terrain characteristics. The final goal of this step is to find age-pattern relationships.

The terrain characteristics of perfect banded patterns have been used for the analysis, as they were the easiest to recognise. The age map is reclassified to 20 intervals of 500 years each and clipped with a hummock landcover map of which the confidence of classification is 50 percent or higher. A stratified random sampling of points is then used per age interval. The pattern metrics and terrain characteristics of these points are then analysed with various techniques and programmes (Table 4.3). Fast Fourier Transfer (FFT) autocorrelation, spa-
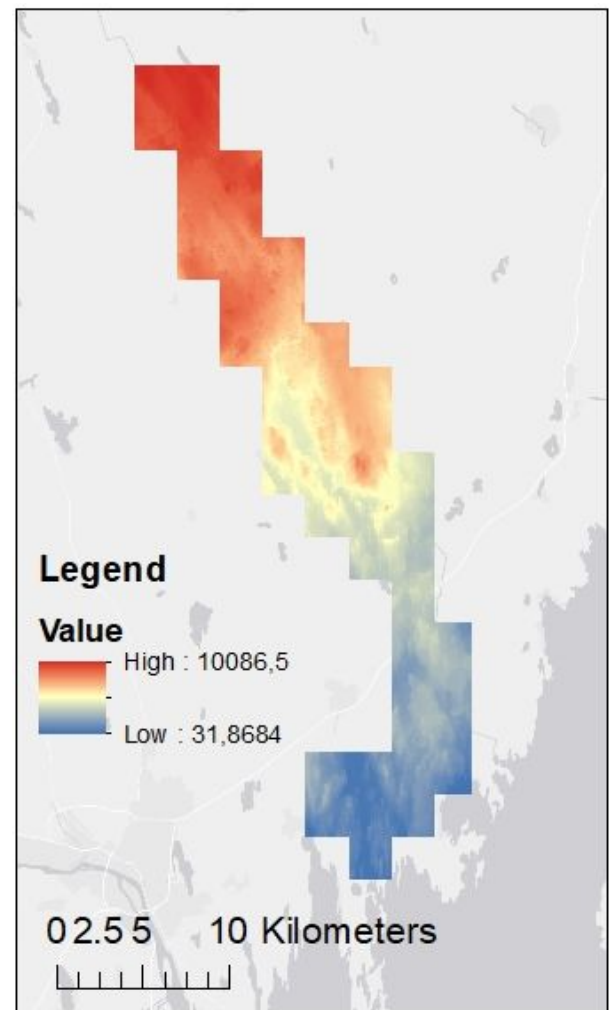
Figure 3.4: Map showing the age of the landscape, based on calculations with the DEM and the shoreline displacement curve.

tial early warning matrices and FRAGSTATS metrics will be calculated for each point, and are dependent on the terrain, hence will be called dependent variables. The terrain characteristics are calculated with SAGA GIS in R (RSAGA package, Brenning (2008)), using the DEM as input, for the same points, and are called independent variables (Table 3.3). All the terrain characteristics that could be calculated were chosen for the analysis. There

was no preselection of which matrices would be used. This step will provide a measure of quantifying 'patterness' -how much and what kind of patterns- in relation to the environment (i.e. terrain).

A point will have multiple pattern and terrain characteristics. The next step is to fit the independent and dependent variables in a Generalized Additive Model with integrated smoothness estimation (GAM), and finally, using R^2 to sort the variables, find the best 100 relationships. The advantage of GAM is that it can deal with highly nonlinear relationships (Guisan, Edwards Jr, & Hastie, 2002). Both pattern-age, as well as pattern-terrain relations, will be quantified in this last step.

Validation

Validation has been done on landcover classification, and for the youngest peatlands, on age. Landcover classification has been done by visual inspection of the classes, and with a confusion matrix, kappa's statistics and accuracy assessment. The age has also been calculated for the points of the field data, based on the shore displacement curve and compared with the measured age of the field data. The average calculated age is 270 years (range: 145-356 years) older than what was measured from the field samples (Figure 3.5). This means that the calculated age is older than what was measured.
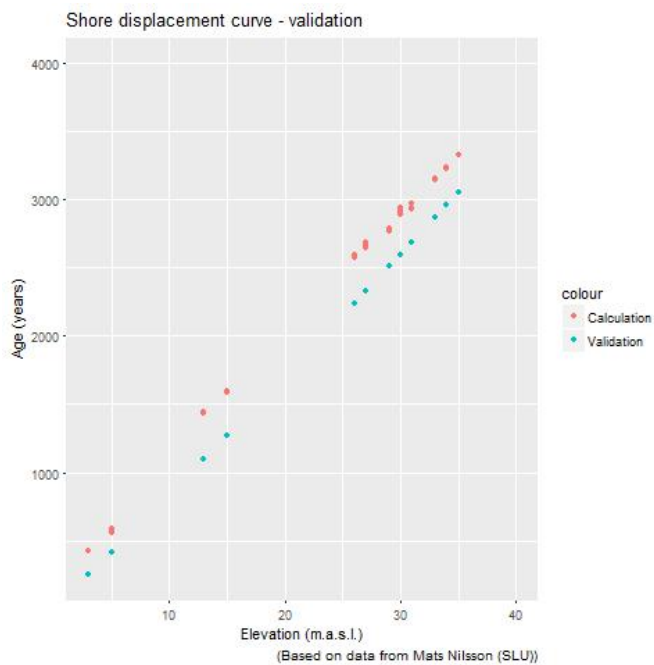
Figure 3.5: Validation of the calculated shoreline displacement curve. Calculated values are based on the shoreline displacement curve, the validation values are based on field measurements by Mats Nilsson.

4 | Results

This chapter will discuss the quality of the land cover classification and its sensitivity to classification input in Section 1, as well as the pattern-age relationships in section 2.

4.1 Land cover classification

These first results will show examples along the transect and the classification accuracy. Next, a sensitivity analysis is shown, where different elevation and spectral bands were used for the classification.

4.1.1 Peatland patterns along the chronosequence

As previously mentioned, two separate landcover classification maps have been prepared. The reason to make two classification maps was that due to the difference in acquisition date, spectral characteristics of the images for these two dates differed and peatland classes could not be classified based on one signature file. The resulting classification datasets are not the same size: the July dataset is almost four times larger than the May dataset (Table 4.1). The percentage of the area classified as hummock, hollow and water is comparable in both classifications. However the mudbottom and sedge class are not. The May dataset has more mudbottom than sedge, while July has it the other way. The reason for this difference in the area can be that in May the vegetation (sedge) has not recovered from the winter period yet, and as such has not grown out of the mudbottom, in which it grows. The composition of landcover also changes for different age classes (Figure 4.2). As peatlands develop, the amount of sedge decreases, while hummock increases. Hollows also increase, however, their percentage of land cover varies a lot with each age class. The amount of mudbottom remains stable, except for the 1000 years. Figure 4.2 also shows that water is hardly classified at all, only in two age classes.

Table 4.1: Total classified area per category, in pixels, hectare and percentage of total. The May dataset is smaller than the July dataset (almost 25%).

The overall result shows large surface areas of hummocks and hollows (Figure 4.1), with a few sedge areas in the southern part of the transect. It also appears peatlands are more extensive in surface area when going land inwards (and being older). However, this may be caused by one of the first steps in selecting peatlands and dividing them up into smaller peatlands. Watershed boundaries may cut a peatland in half (Figures 4.3g&h), and peatlands may have been excluded because of a small parcel of agriculture in the catchment. Near the coast, there is also more agriculture than farther land inwards.
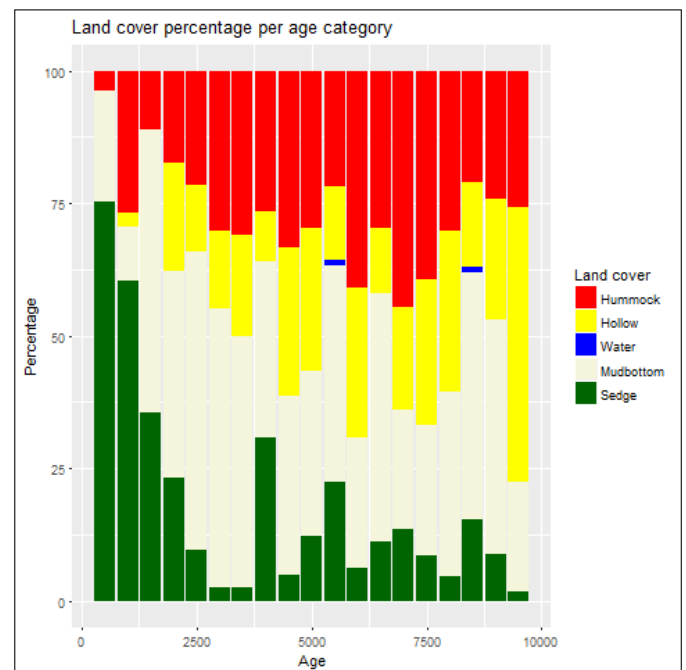
Figure 4.2: Landcover (in percentage) per age category of 500 years. Sedge decrease with age while hummocks and hollows increase.

To evaluate whether patterns occur and how they change along the transect, five peatland sections of different age groups (8600, 6000, 5100, 3000 and 1800 years old) are subjected to closer inspection (Figure 4.3). This age is based on the glacial rebound calculation. The transect was divided into five sections for the five age categories, and per section, a visual scan was done to find a representative peatland.

The hummock-hollow patterns are seen clearly by the red and yellow colours, respectively. On all five RGB images of the peatlands, there are patterns or hummock patches visible, and in general, these patterns are well-reproduced on the classification map. Furthermore, older peatlands (Figures 4.3a-d) seem to have more patterns as compared to the youngest peatland (Figures

	May		July	
	Area (ha)	% total	Area (ha)	% total
Hummock	153	23.0	576	29.4
Hollow	119	18.0	398	20.3
Water	4	0.5	2	0.1
Mud	336	50.8	646	33.0
Sedge	51	7.7	336	17.2
TOTAL	662	100	1958	100

Figure 4.1: *Landcover classification over the whole transect. See Annex B for more detailed maps.*

4.3i&j). The scale of these (older) patterns is also larger than on younger peatlands.

Going into more detail, the two oldest peatlands (Figures 4.3a-d) show similar patterning, with thick bands in string and maze patterns. On the edges, near the forest, the hummocks either clump together to form a plateau, or get sparser, and hollows or mudbottoms remain. The middle-aged peatlands (Figures 4.3e-h) show fewer hummock bands than in the previous examples, but they are still present. Another similarity is the plateau forming near the edges in some cases. On the other hand, there are more disconnected patches of hummocks, with much more area classified as hollows and mudbottoms. In the youngest peatland (Figures 4.3i&j) there are no banded patterns of hummocks. Instead, there are many small disconnected patches.

4.1.2   Classification accuracy

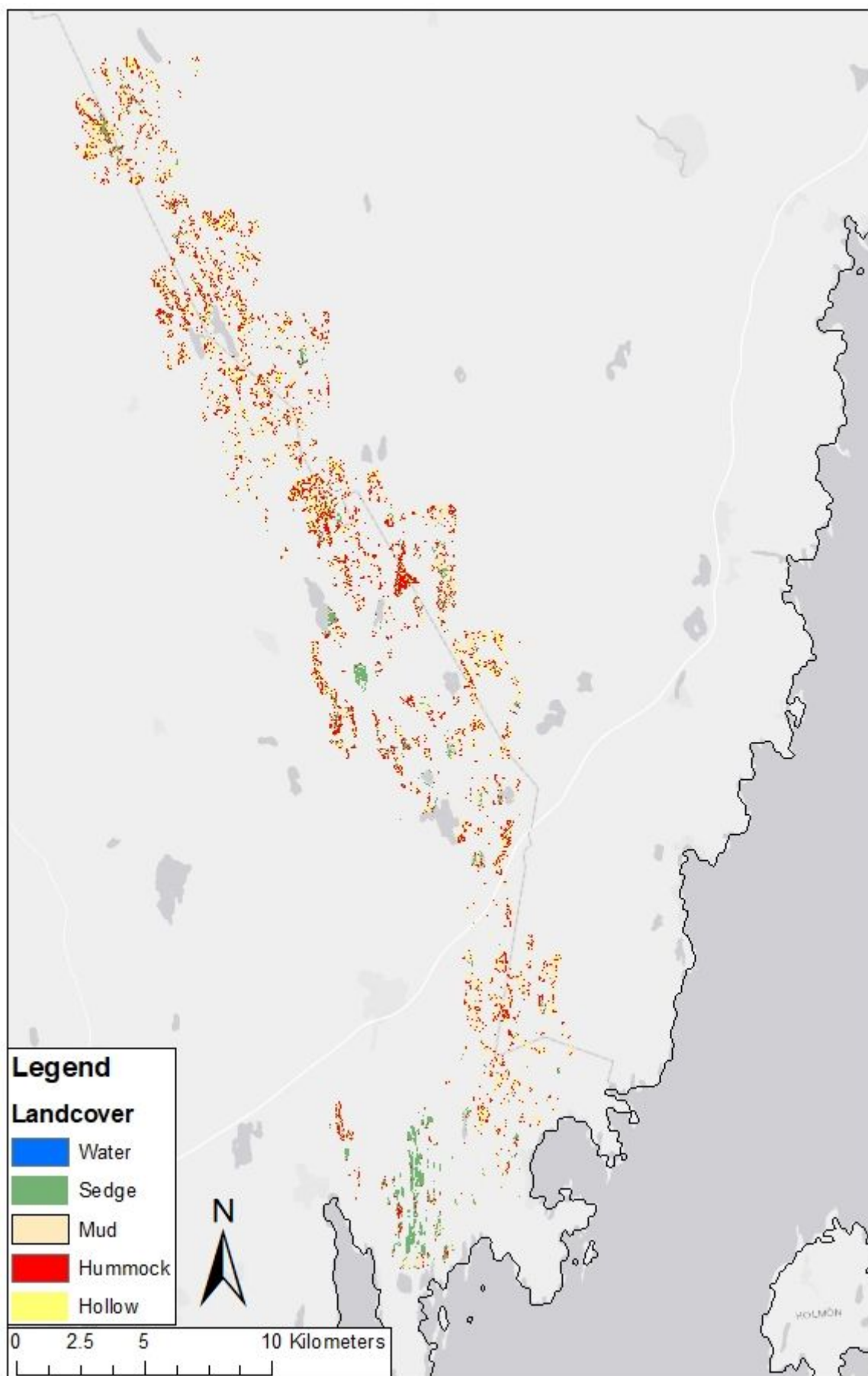The overall accuracy of the classification was 100%, based on 21 validation points for the study area, with a Kappa statistic of 1 (Annex D). This was the same when using different local DEMs as input for the classification, and spectral bands.

Although no misclassification occurred at the points evaluated, close visual inspection indicates that vegetation cover type and pattern contain errors outside the evaluated points. Figure 4.4 shows an example for which an apparent homogeneous peatland, as can be observed from the RGB image, is classified in hummock, hollow and mudbottom classes. One possible reason for this subdivision is the variation in elevation as represented by the variation in the local DEM. Homogenous hollows or mudbottoms are present throughout the area, and the classification such as the example occurs in half of them. In the other half, these are classified as homogenous areas.

A second example is comparable, the RGB image of Figure 4.5 shows a relatively homogeneous hummock which contains a track, with a slightly lower local DEM than the surroundings. The resulting classification shows a more substantial hollow cover in the path through than observed in the RGB imagery. There are not many peatlands with tracks like these in the study area. However, there are some drainage canals present in a few. These are mostly classified as two straight parallel lines of hummock with sedge in between. This is more frequent in the southern part (younger peatlands) than the northern part of the study area, due to more urbanisation, but it is still absent in most peatlands.

Finally, a third example shows how the two classifications merged. Figure 4.6 shows the acquisition date border with July on the left and May on the right, which covers one peatland. The water in May appears darker, whilst it is greener in July due to vegetation growth. The other vegetation is also greener in July than in May, which is the remaining snow from the winter. In July, nearly all vegetation is classified as sedge, while in May there is much more mudbottom and a few hummocks. In some places there is a seamless transition, from sedge to sedge, while other sites have a sharp change from sedge to hollow. There are only a few areas where the acquisition date border crosses over peatlands such as with the example, thus it is not very representative for the whole study area.

4.1.3   Sensitivity of classification results to local DEM input: 10 vs. 20 vs. 30 m

The examples from the previous section have shown that the local DEM influences the classification (Figure 4.6-4.5). The local DEM indicates local elevation differences and requires the focal range to be set. To test the sensitivity of this setting, three focal ranges have been used, namely 10, 20 and 30 meters. In the example peatland (Figure 4.7a) hummock strings surround a few small pools and a mudbottom. Some of these hummocks are isolated, while other strings come together to form a plateau, which then gradually changes into forest (top, left and right of the peatland).

Besides that, the three local DEM inputs show different elevation ranges (Figures 4.7b-d), there are similarities. Isolated hummocks are classified the same (Figures 4.7e-g, middle of peatland), and the widths of hummock strings are comparable, although larger focal ranges result in broader patterns. On the other hand, small isolated elevation differences are filtered out as well with larger focal ranges, resulting in less spotty classification (see centre of peatland). A third difference is where the individual strings come together to form a plateau (top, left and right of peatland). With a small focal range, the local depressions within these plateaus are big enough to be classified as hollows, while they should be classified as hummock. Larger values for the focal ranges do not show this. The classification of hollows is also affected by the focal range, with a larger range leading to fewer hollows. Finally, the classification of water is different with the different focal ranges (two small water bodies in middle of peatland).

The actual classification is done with a local DEM of 30 meters. The majority of the hummock-hollow patterns was the same for the three focal ranges, however, differences occurred in the more hummock plateaus. Although they are relatively homogeneous, there are still hollows on them. Another difference is that small focal ranges will show all microtopography, such as a single grass sod, which will be classified as hummock. The local microtopography is filtered out with larger focal ranges.

4.1.4   Different spectral band input: infrared vs. red

Next, to the local DEM, the selected spectral bands as classification input also influence the final classification. This section illustrates how infrared (IR), red (R), or both, in combination with green, blue and a local DEM of 30 meters on local objects affect the classification.
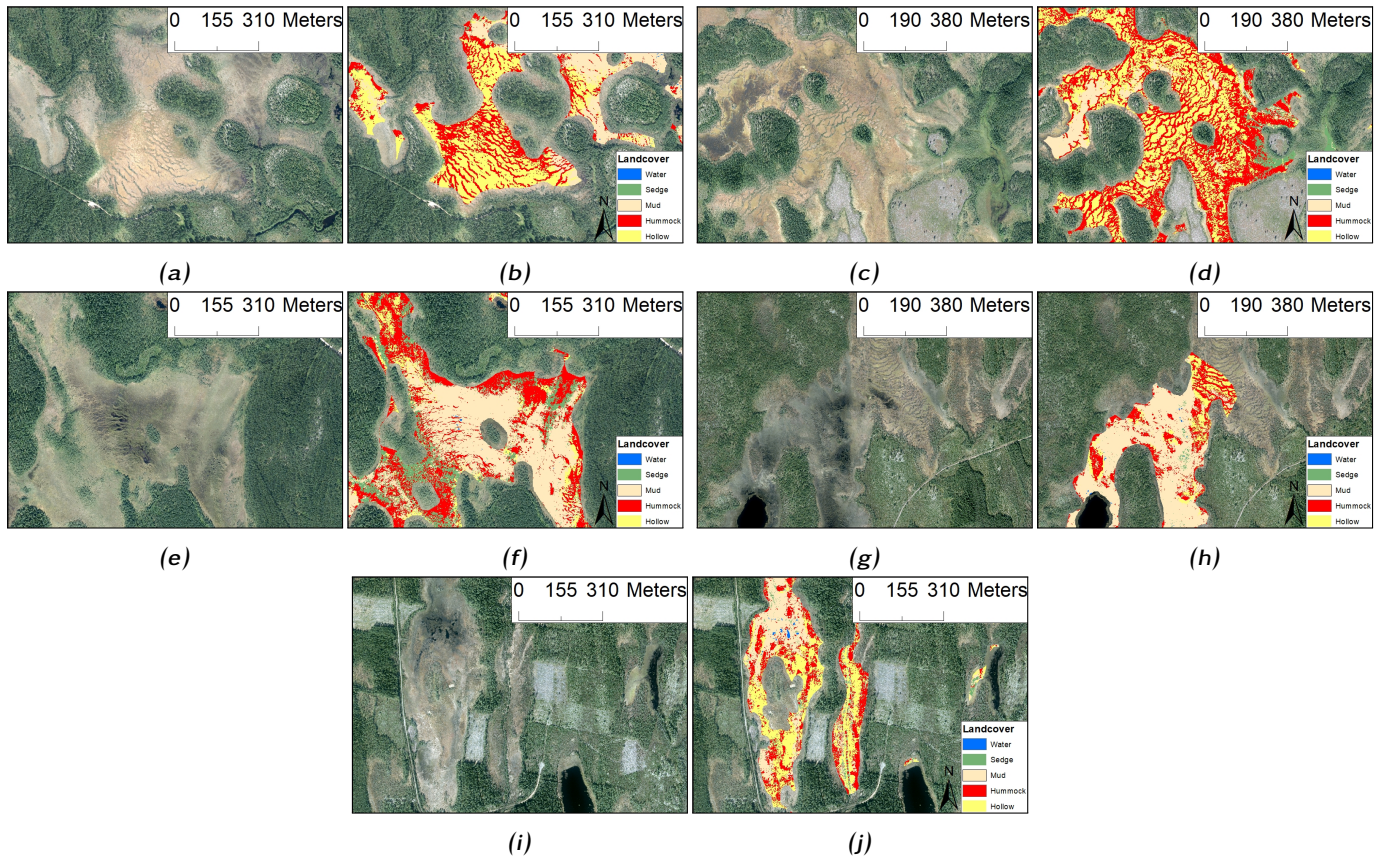
Figure 4.3: *Land cover classification of five peatlands from different age classes throughout the transect: a and b: 8600 years; c and d: 6000 years; e and f: 5100 years; g and h: 3000 years; i and j: 1800 years.*
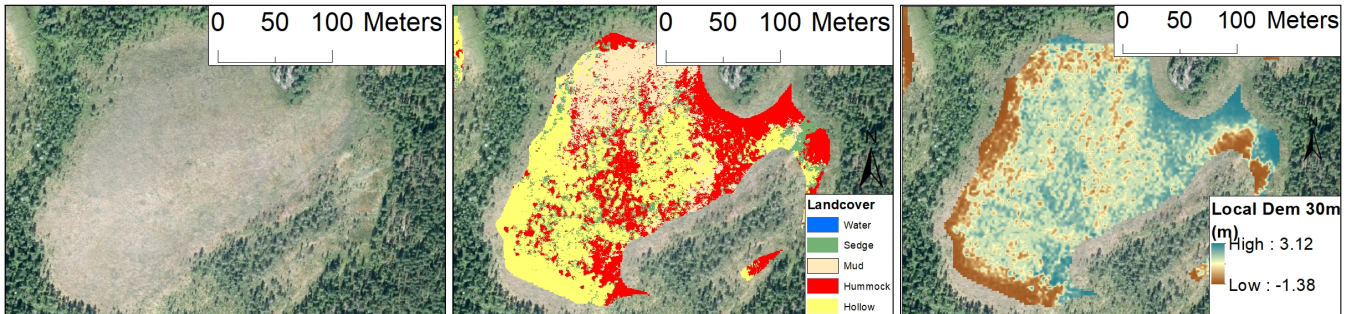

Figure 4.4: *Example of landcover classifications with deviating patterns due to local DEM differences in a homogneous peatland. From left to right: RGB, classification and local DEM.*

Differences are mostly visible in the classification of water and the homogenous hummock plateaus (Figure 4.8), although differences are not big.

When using red (Figure 4.8b) and the combination of red and IR (Figure 4.8d), an equal number of pixels are classified as water, which are divided over a larger and smaller pool in the centre of the peatland. The classification with IR (Figure 4.8c) only shows one pool, which is also smaller than in the other classifications. The majority of the hummock strings is classified in the same way, for all three inputs, with comparable widths and lengths. The variances occur in the more homogenous areas (top, left and right of the peatland).

Using red results in more homogenous plateaus, while both IR and the combination of the two show hummocks with hollows in between. Although these plateaus

are present in individual peatlands, they are not as predominant as shown in Figure 4.8b. One other difference with the inputs is the sedge class. In the top left of the images, there is a small stroke of sedge class, which is largest for the IR based classification and smallest for the combination.

4.2 Spatial vegetation patterns throughout the transect

The points that have been selected for the pattern analysis were based on a hummock classification confidence of over 50%. Of all the pixels, only 8% of the May dataset and 4% of the July dataset were classified with over 50% confidence (Table 4.2) to begin with, for all classes How much of this is hummock has not been calculated.
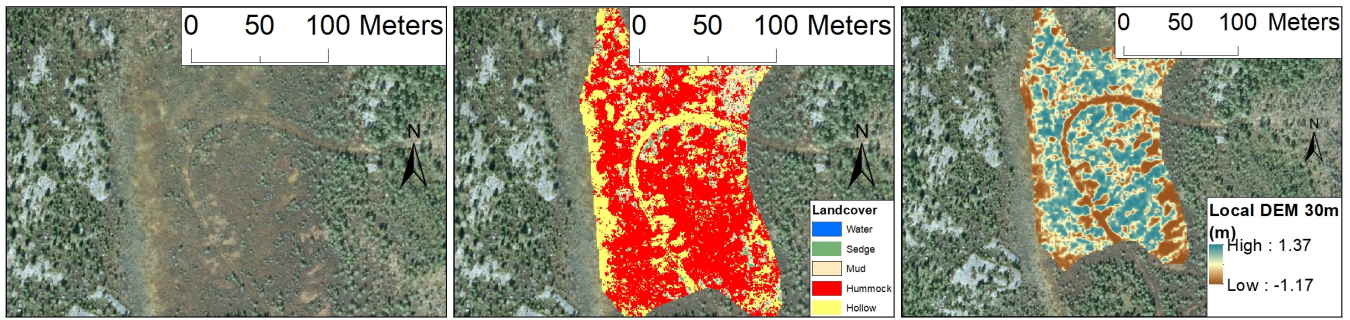
Figure 4.5: Example of landcover classifications with deviating patterns due to local DEM differences. A track is classified as hummock, which should be classified as hummock for the majority of the area. From left to right: RGB, classification and local DEM.
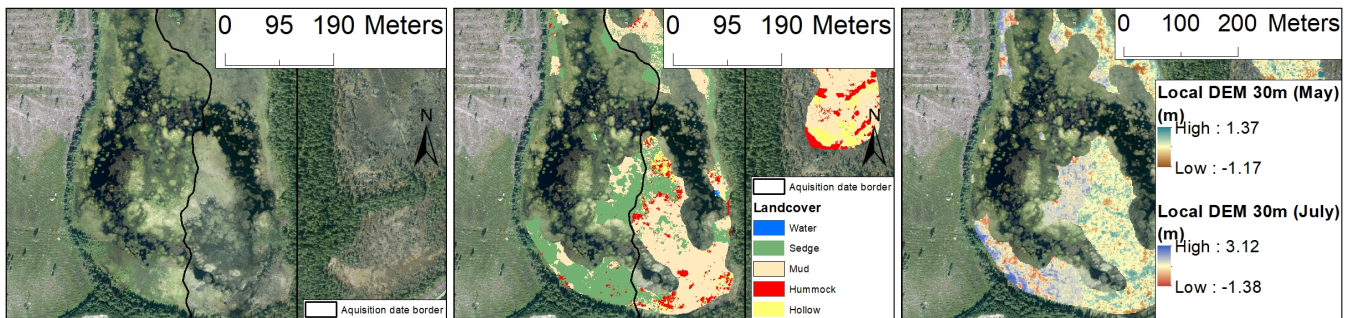

Figure 4.6: Example of landcover classifications with deviating patterns due different signature files, July on the left and May on the right. From left to right: RGB, classification and local DEM.

Table 4.2: Certainty range of classification confidence and how many pixels were classified in that range. Levels are based on the maximum likelihood classification tool.

Value	Certainty	May % of total	July % of total
1	.995 to 1	0.13	0.07
2	0.99 to 0.975	0.12	0.06
3	0.975 to 0.95	0.38	0.21
4	0.95 to 0.9	0.70	0.36
5	0.9 to 0.75	1.43	0.77
6	0.75 to 0.5	5.12	2.70
7	0.5 to 0.25	11.95	6.23
8	0.25 to 0.1	19.61	10.88
9	0.1 to 0.05	19.55	13.99
10	0.05 to 0.025	9.99	9.70
11	0.025 to 0.05	6.91	8.73
12	0.01 to 0.025	6.72	10.91
13	0.005 to 0.01	3.54	6.83
14	<= .005	13.86	28.57
	Total	100	100

4.2.1 The minor range development through time

Despite the vast diversity along the transect, an r^2 of 0.26 was obtained between age and minor range of patterning. This metric has the highest correlation with age. The GAM analysis suggests that the minor range peaks at an age of around 6-7000 years, after which it decreases again (Figure 4.9). This indicates that hum-mock bands increase in width until a maximum width is achieved, after which it the bands gets narrower as the peatland gets older. Despite this trend, there is a considerable variety in the data, especially with higher ages. At the same 6-7000 years peak, the minor range can be from anywhere between just above 0 as to over 40 meters. Nevertheless, young peatlands don't have high minor ranges, meaning this metric can be used to detect old peatlands.

Not all points are used for this GMA. Data is missing on minor ranges at ages before 2000 years and between 3000 and 6000 years. That is because of the chosen radius for the fast Fourier transform (FFT) which is set at 30 meters, and the minor range is calculated with the FFT. A buffer is placed around the points, and if there are places with 'no data' present in the 60 by 60 bounding box the points are excluded from analysis.

Figure 4.9 further shows what the hummock-hollow patters look like at specific points. For example, older peatlands (#85, #98, #110, #91 and #62) show more bands than young peatlands (#7 and #25). Higher minor ranges (#85 and #98) also show wider bands than low minor ranges (#62 and #91).

4.2.2 The radius of gyration development through time

An r^2 of 0.128 was obtained between the standard deviation of the radius of gyration and age (Figure 4.10). The radius of gyration is the distance between each cell of a patch and the patch centre. This metric increases with age according to a linear relation. What this means is
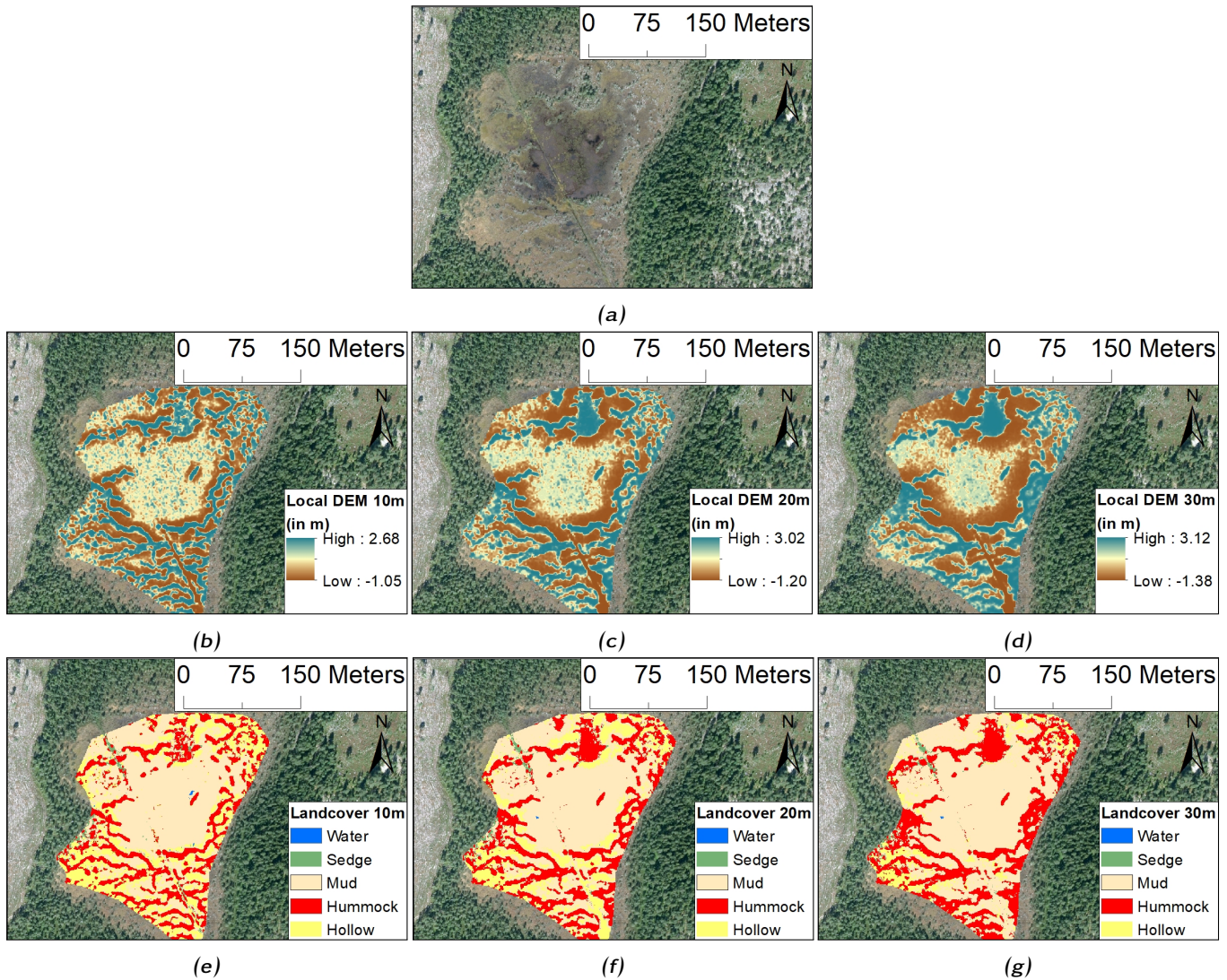
Figure 4.7: *Influence of different local DEM ranges on classification result of a peatland (a: RGB image), with b: 10m; c: 20m; and d: 30m focal range. Classification results are shown in e,f and g.*

that the patches become bigger as a low radius of gyration occurs with young peatlands, while older peatlands have higher values. Although there is a positive relation, there is variation in the data, although most of the higher values occur with older peatlands. This GAM has more points than the previous GAM (Figure 4.10) because this metric is calculated with a different method that does not exclude areas with no data.

The classification examples in Figure 4.10 show that a low radius of gyration is expressed by small patches, without a specific shape. As the radius value increases the patches rapidly form banded patterns, which grow in length as well. However, there are also peatlands between 3000 and 4000 years old that still have a low radius of gyration, although there are no older peatlands with this low value.

4.2.3 The perimeter/area ratio development through time

The age perimeter-area ratio GAM has an $r^2 2$ of 0.116, with a decreasing trendline (Figure 4.11). This metric

shows that older peatlands have lower perimeter-area ratios than younger peatlands. What this means is that if the shape of the peatland is kept constant, an increase in the area will mean a decrease in the perimeter-area ratio. This can mean that hummock patches grow into plateaus, or into long, broad hummock bands. High perimeter-area ratios do result in small patches of a few pixels.

The classification examples in Figure 4.11 show that a low parameter/area ratio is expressed by large patches (#70), however similar ratios can also be expressed in many connected strings of hummocks (# 29 and #110). Young peatlands have high ratios, which result in many small, disconnected patches that grow together as the peatland grows older.

4.2.4 Other age-related metrics

More correlations have been made between pattern metrics and age, and all have linear relationships (either positive or negative). The GAM figures can be found in Annex E. The Contiguity Index increases with age,

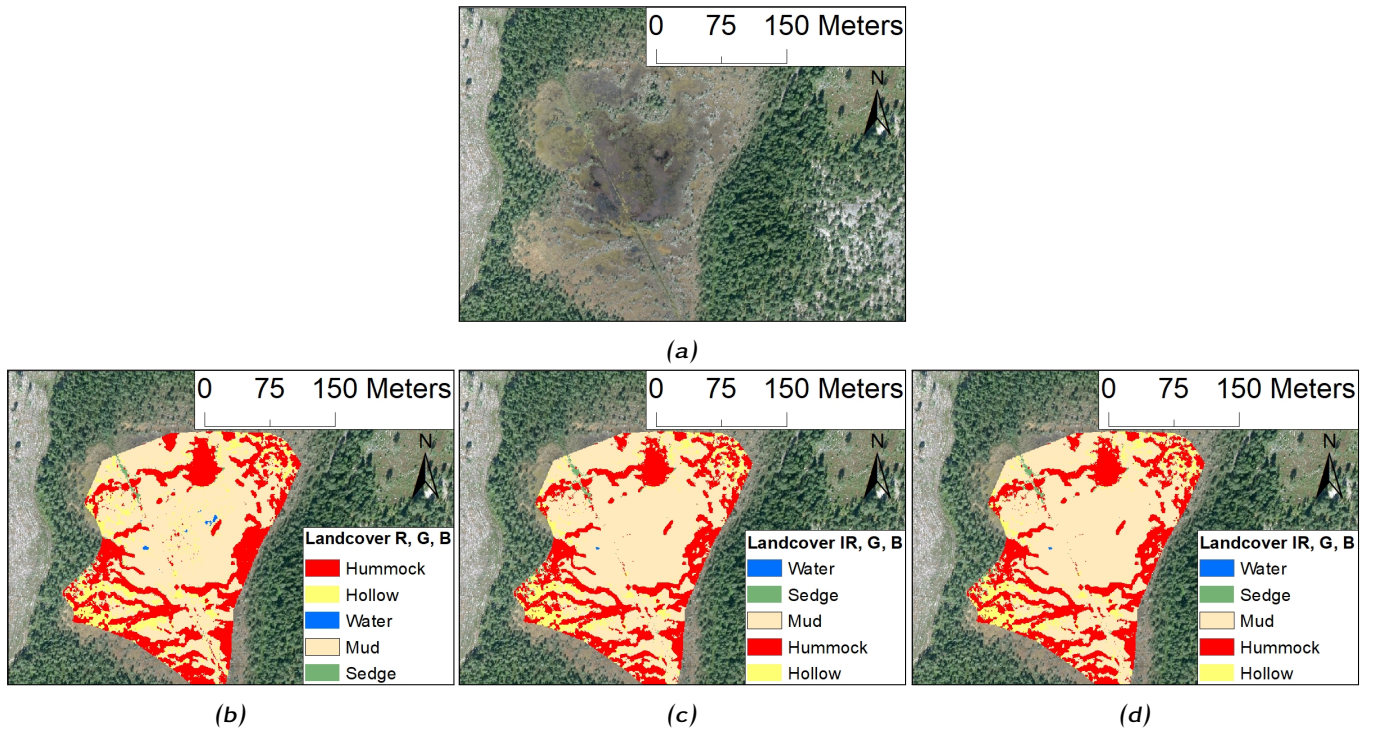**Figure 4.8:** *Influence of different red spectral bands on classification of a peatland (a: RGB image), with either red (b), infrared (c) or both (d) as input.*
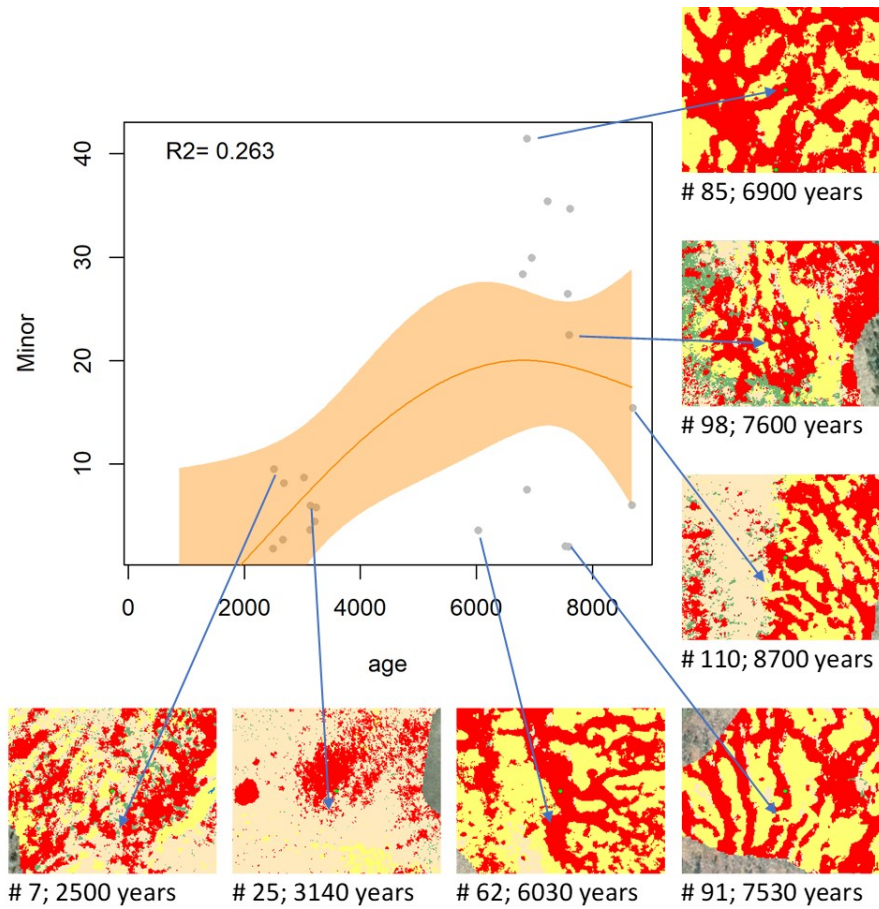

Figure 4.9: *Age-Minor range correlation, with 7 field examples. The classification images are 120 meters wide, 60 meters high. Colours correspond to previous classification legends: red = hummock; yellow = hollow; green = sedge; beige = mudbottom; and blue = water.*
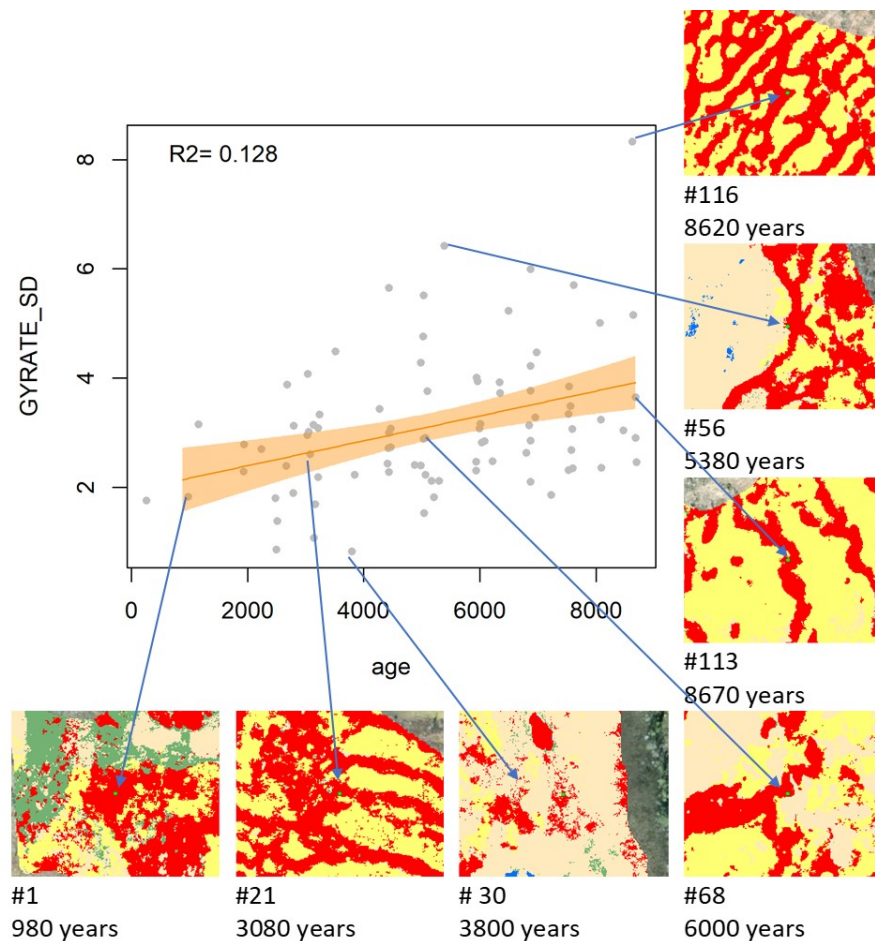
Figure 4.10: *Age-radius of gyration correlation, with 7 field example. The classification images are 120 meters wide, 60 meters high. Colours correspond to previous classification legends: red = hummock; yellow = hollow; green = sedge; beige = mudbottom; and blue = water.*

Table 4.3: *The same metrics that were correlated with age are also correlated with these terrain characteristics . Total catchment area and slope length have the most correlations. X shows which correlations are presen, - shows no indication. Gyrate = radius of gyration; para = perimeter/area ratio; contig = contiguity index; LSI = landscape shape index; pladj = percentage of like adjacencies; ai = aggregation index; np = number of patches.*

	Gyrate+area	Para	Contig	LSI	Pladj+ai+np	Minor+major
Total catchment area	X	X	X	X	X	-
Slope length	X	X	X	-	-	-
Openness (positive)	X	-	-	-	-	X
Flowpath length	X	-	-	-	-	-
Aspect	-	X	X	-	-	-
Downslope distance gradient	-	-	-	X	-	X
Slope	-	-	-	X	-	-

meaning patches become more connected, as does the Percentage of Like Adjacencies, which is 100 when the landscape is one single patch. The Number of Patches decreases as peatlands grow older, due to the patches growing together, which is confirmed by the area increasing. The Landscape Shape Index also decreases, which reaches a value of one when the landscape consists of a single compact patch.

4.3 Landscape positions of spatial vegetation patterns

The same metrics that are correlated with age can also be correlated with terrain characteristics (Table 4.3). The table shows that the total catchment area above a peatland is correlated with the most pattern characteristics (indicated with *X*), while slope has the lowest. The minor and major ranges are only correlated with the terrain openness and downslope gradient. This table is just meant to give a first impression of possible relations. An-

Figure 4.11: *Age- perimeter/area ratio correlation, with 7 field example. The classification images are 120 meters wide, 60 meters high. Colours correspond to previous classification legends: red = hummock; yellow = hollow; green = sedge; beige = mudbottom; and blue = water.*
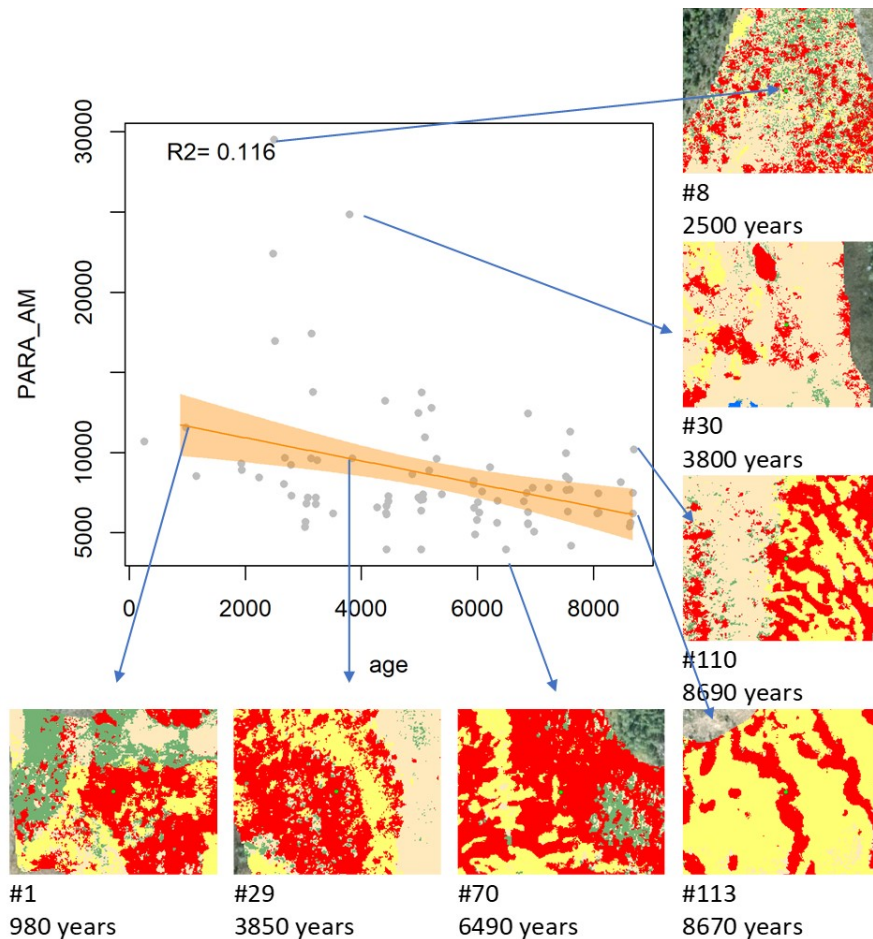
nex F shows additional GAM charts for an illustrational purpose, with how the metric values can be seen in the classification map.

Terrain mostly influences the hydrology, and thus also nutrient flow. What most of these terrain characteristics indicate is how water flows. Total catchment area, for example, calculates the flow accumulation based on the DEM, from highest to lowest cells. Slope length is also based on the distance from the highest to the lowest cell: based on neighbouring cells with the steepest gradient, until the slope of a neighbour is less or equal than the currently processed cell. The Topographic openness expresses the dominance (positive) or enclosure (negative) of a landscape location, so how wide a landscape can be viewed from any position. The downslope distance gradient quantifies downslope controls on local drainage. Aspect is not hydrology related though; it shows the orientation of the slope.

5 | Discussion

This paper studied whether open-source aerial photographs can be used as a basis to identify and analyse spatial vegetation patterns in peatlands. Overall, these patterns were detectable throughout the transect, which could then be used to analyse the peatlands, particularly older peatlands (over 2000 years).

5.1 Peatland age and pattern development

This study used metrics to quantify the pattern development in peatlands. The results show that the minor and major range were the most important metrics, followed by the radius of gyration and the perimeter-area ratio (Figures 4.9, 4.10 & 4.11). The values of these metrics increase as the peatlands increased in age (except for the perimeter-area ratio, which decreases). The hummock patches increase in width, length, and area and patches become less isolated as they grow together.

Pattern change in the Everglades (Florida, USA) was analysed using length/width and perimeter/area metrics (Nungesser, 2011), while a bog in Austria was analysed using class area, mean patch size, number of patches, total core area, number of core areas and proximity index (Langanke, Burnett, & Lang, 2007). In Argentina, Herrera, Laterra, Maceira, Zelaya, and Martínez (2009) and Argañaraz and Entraigas (2014) used the largest patch index, mean patch size, patch-size coefficient of variation, landscape index and Euclidean nearest neighbour distance to analyse grasslands. This tells that there are no straightforward metrics for examining landscapes.

A critical point for the evaluation of the pattern development is the adopted sampling strategy, which was to stratify random sample points over the transect, in age categories of 500 years, on hummocks that were classified with over 50% confidently (Table 4.2). Although the peatlands of 2000 years and older had enough hummock to do this, the younger peatlands did not. This means that the current sampling strategy does not consider the young peatlands sufficiently as visually examining the young peatlands (Figure 4.1) shows that there are hummocks present. This means that the confidence level of the classification is too low to be considered acceptable (Table 4.2). A low confidence level can also mean that the classification itself needs improvement (i.e. the signature file).

So either a different sampling strategy is needed to include these young peatlands, or young peatlands did not have enough time yet to develop sufficient hummock patterns that can be classified confidently. In their study, Mathijssen et al. (2017) examined a peatland in

Finland and found that the whole peatland went through the same succession phases (from rich fen-poor fen-bog), however various parts of the peatland transitioned at separate times. Their peatland started as several smaller ones, which merged to form a bigger peatland, with the older centre being poor fen while the outsides were rich fens. This process took approximately 2000 years, which indicates that the younger peatlands (< 2000 years) in the study area may still be undergoing this same process. Klinger (1996) also mentions that succession from forest to bog occurs over a period of at least 2000 years.

Young peatlands near the coast may still be undergoing this process, but more land inwards there are also peatlands which have the same visual characteristics as these young peatlands. But, according to the age calculation, they are recognised as older than 2000 years (Figure 4.9). This may suggest that peatlands don't always follow the same succession path from rich fen to poor bog, even within the same area. However, there is a theory in which successional pathways converge from forest to stable climax bogs (Klinger, Elias, Behan-Pelletier, & Williams, 1990; Klinger & Short, 1996) making this idea is unlikely.

Glaser, Hansen, Siegel, Reeve, and Morin (2004) mention that the isostatic uplift, rather than climate, was the principal driver of peatland development in the Hudson Bay lowlands, in Canada. The slope is continuously reduced because of this uplift, changing drainage (or even impeding it) and river gradients. As a result, new areas become waterlogged and growth of peat is initiated. Consequently, these new peatlands are classified as old peatlands because of their location, instead of being classified as young. Tuittila et al. (2013) also found that external forces (isostatic rebound) led to different rates of peatland development on the west coast of Finland, in the Gulf of Bothnia. There is also literature suggesting that speed of succession, and thus hummock-hollow pattern development, may depend on climate and catchment hydrology: in cold climates, the fen stage persists, which are usually also old, while bog stages are reached in warmer climates Väliranta et al. (2017). Considering that the transect is only 40 km long, this last theory is unlikely.

Besides the age, there were also terrain characteristics correlated with pattern metrics (Table 4.3). Many of these terrain characteristics were somehow related with each other as well, as could be seen in the similar GAM trendlines, and the correlation matrix between pattern metrics and terrain characteristics (Annex G). A lot of literature mentions the string-like hummock patterns appear on slopes, however, this research found

that slope did not have the highest correlation (Annex F). Instead, the total catchment area above peatlands showed the most correlations with metrics (Table 4.3). This terrain characteristic does contain aspects of other terrain characteristics, as a high total catchment area can only be achieved if all upslope water passes the point of measurement. Hence the point must be on a slope, which must be long. Thus, the slope and slope length are indirectly considered in this characteristic. There are more terrain characteristics like this, however, this research has not focussed on how they are related, and which ones complement each other.

5.2 Landcover classification within the peatlands

Analysing the development of peatlands and their patterns with aerial imagery can be challenging, therefore within the peatlands, five different classes were defined for more unambiguous interpretation. As a comparison, Poulin et al. (2002) used 13 habitat classes for peatlands, basing the training sites on three experts who could recognise patterns on aerial photographs, including spruce forest. Anderson et al. (2010) used ten categories, including woodland and grassland, to classify peatlands. Although using more classes give more information, it also increases the confusion between classes. In their paper, Poulin et al. (2002) state that three similar classes seemed easily confused within their study. Anderson et al. (2010) also mentioned misclassification of categories, due to similar vegetation types, or features being smaller than the spatial resolution. In hindsight, for this research, the mudbottom class would maybe have been better classified if it was split up into lighter and darker mudbottom; however, more classes are not needed.

Determining which locations should be selected for the signature file of the classification greatly determines the classification results (Ok & Akyurek, 2011). That is because each defined class will have their range of values in the colour spectrum and local DEM. If there are points of two classes that have overlapping ranges, the classification procedure will include some confusion as it needs to decide which of the two classes will be used. The identification of hummock-hollow patterns in this research is done by adopting a supervised maximum likelihood classification. The supervised aspect is related to the point selections for the signature file, which were manually placed along the transect. There is a bias towards hummocks in this study, as the points for this category were placed and optimised iteratively to include as many hummocks as possible, while other categories received less attention. This is because hummocks are the focus group for the pattern metric calculations, and they are the easiest to identify from the aerial imagery visually. The two sensitivity tests further showed that the local DEM in combination with colour (Figure 4.7) had more influence on the classification than using different spec-

tral bands (infrared/red), especially for the hummocks (Figure 4.8). This is probably because the classification points were placed on high values of the local DEM.

Although the classification accuracy was 100%, this was only based on 21 points. These 21 were randomly selected from the 104 initial points used for classification, and the sample size is expected to be too little. Therefore, the visual inspection was also done. Through this, some instances of landcover misclassification have been found, for example in homogeneous peatlands (Figures 4.4 & 4.5). The acquisition date of the aerial images also had an important influence on the classification (Figure 4.6), as the greenness between both data sets is different and two different signature files for the two different acquisition periods are required to prepare an accurate classification. Even though the classification results were combined eventually, it is easier to use one acquisition date and focus on that, than trying to combine.

The classification methodology in this research suggests that supervised MLC is a suitable way to analyse peatlands. MLC is also considered suitable for peatland classification by Poulin et al. (2002). All data sources are maintained and kept up to date by either the Swedish cadastre of hydrology department. The only involvement is with the supervised sampling strategy for MLC and the analysing of patterns steps.

5.3 Relevance of this research

This research has shown that pattern development in peatlands can be recognised and quantified by using areal imagery, over a large area. Wetland classification using remote sensing has been done for a long time, but kicked off after the development of satellite remote sensing (Guo, Li, Sheng, Xu, & Wu, 2017), although most research that used areal imagery was used for small wetland areas or used to assess the classification results of remote sensing techniques with low resolution. However, for peatlands a fine scale resolution is recommended, due to the processes and patch sizes (Aplin, 2006), placing more focus on the use of aerial imagery for peatland classification. The resolution should be fine enough to include the studied features, so for studying hummocks and hollows, the resolution should not be much larger than 0.5m.

Besides being able to understand the pattern development in peatlands, combinations of terrain characteristic values and pattern metrics can be used to predict *where* certain peatlands (i.e. patterns) will be in the landscape. If it is then also known which patterns indicate a nearing catastrophic shift, these peatlands can be prioritised for monitoring this process.

6 | Conclusion & Recommendation

This research aimed to understand the spatial vegetation pattern development through time, using high-resolution images for a chronosequence of peatlands. These patterns were classified using supervised maximum likelihood classification and analysed using various pattern metrics based on hummock patches. Based on the results, the aerial images can be used to classify peatlands into five classes, which can then be quantified using pattern metrics. The hummock patches start off as small clumps of patches when the peatland is young, which grow together to form elongated patches as the peatland grows older. This can be seen in the aerial images and its' classification when going land inwards from the coast, as well as in the GAM figures. The minor and major range of the patches had the highest correlation with age, followed by the radius of gyration, which all increases with age. The fourth best correlation with age was the perimeter-area ratio, which decreased with age. Of the used terrain characteristics, the total catchment area above a peatland influences the pattern development the most, followed by the slope length above the peatland. There is a large variation in patterns and where in the landscape they develop, which also results in weak relationships.

Although the result showed that patterns change throughout the transect, the peatlands younger than 2000 years were underrepresented in the applied sampling strategy. This was caused by an insufficient presence of hummocks in the young peatlands, which were used in the pattern analysis.

This study was of an explorative nature, i.e. trying to understand the peatland development through a combination of aerial imagery and pattern metrics. Experiences from the past research and recommendations will be mentioned here.

I The methodology of this research can show where potential peatland patterns may develop in the future, based on where current hummock patterns are located in the landscape (i.e. terrain characteristics). A next step could be to further determine in what terrain characteristic ranges these patterns occur and to select peatlands within those ranges for further analysis. This way the young peatlands are included in the research, even though the hummocks have not developed yet.

II Furthermore, there is not a lot of validation data in the form of fieldwork to verify the age of peatlands, other than a few locations near the coast. Datasets on peatland depths in Sweden are available on https://www.sgu.se/produkter/geologiska-data/oppna-data/jordarter-oppna-data/torvlagerfoljder/, which could serve as a guide for selecting peatlands in future research. Although the actual age is not given, the dept can indicate if peat is old or young.

III Finally, although various metrics can be used to analyse the development patterns, peatlands are still complex systems. Further work should be focussed on understanding the correlations between various terrain characteristic that influence the vegetation pattern development, and which pattern metric combinations may best describe the development stage.

Bibliography

Anderson, K., Bennie, J., Milton, E., Hughes, P., Lindsay, R., & Meade, R. (2010). Combining lidar and ikonos data for eco-hydrological classification of an ombrotrophic peatland. *Journal of environmental quality*, *39*(1), 260–273.

Aplin, P. (2006). On scales and dynamics in observing the environment. *International Journal of Remote Sensing*, *27*(11), 2123–2140.

Argañaraz, J. P., & Entraigas, I. (2014). Scaling functions evaluation for estimation of landscape metrics at higher resolutions. *Ecological informatics*, *22*, 1–12.

Arrell, K., Wise, S., Wood, J., & Donoghue, D. (2008). Spectral filtering as a method of visualising and removing striped artefacts in digital elevation data. *Earth Surface Processes and Landforms*, *33*(6), 943–961.

Belyea, L. R., & Clymo, R. (2001). Feedback control of the rate of peat formation. *Proceedings of the Royal Society of London B: Biological Sciences*, *268*(1473), 1315–1321.

Belyea, L. R., & Malmer, N. (2004). Carbon sequestration in peatland: patterns and mechanisms of response to climate change. *Global Change Biology*, *10*(7), 1043–1052.

Berglund, M. (2012). The highest postglacial shore levels and glacio-isostatic uplift pattern in northern sweden. *Geografiska Annaler: Series A, Physical Geography*, *94*(3), 321–337.

Bergonnier, S., Hild, F., & Roux, S. (2007). Local anisotropy analysis for non-smooth images. *Pattern recognition*, *40*(2), 544–556.

Brenning, A. (2008). Statistical geocomputing combining r and saga: The example of landslide susceptibility analysis with generalized additive models. In *Saga – seconds out (= hamburger beitraege zur physischen geographie und landschaftsoekologie, vol. 19)* (pp. 23–32). J. Boehner, T. Blaschke, L. Montanarella.

Bridgham, S. D., Johnston, C. A., Pastor, J., & Updegraff, K. (1995). Potential feedbacks of northern wetlands on climate change. *BioScience*, *45*(4), 262–274.

Cimatedata.eu. (n.d.). *Cimatedata eu.* Retrieved from \url{https://www.climatedata.eu/climate.php?loc=swxx0038&lang=en}

Clarkson, B. R., Schipper, L. A., & Lehmann, A. (2004). Vegetation and peat characteristics in the development of lowland restiad peat bogs, north island, new zealand. *Wetlands*, *24*(1), 133–151.

De Vleeschouwer, F., Chambers, F. M., & Swindles, G. T. (2010). Coring and sub-sampling of peatlands for palaeoenvironmental research. *Mires and peat*, *7*.

Eppinga, M. B., De Ruiter, P. C., Wassen, M. J., & Rietkerk, M. (2009). Nutrients and hydrology indicate the driving mechanisms of peatland surface patterning. *The American Naturalist*, *173*(6), 803–818.

Eppinga, M. B., Rietkerk, M., Wassen, M. J., & De Ruiter, P. C. (2009). Linking habitat modification to catastrophic shifts and vegetation patterns in bogs. *Plant Ecology*, *200*(1), 53–68.

Foody, G. M. (2002). Status of land cover classification accuracy assessment. *Remote sensing of environment*, *80*(1), 185–201.

Glaser, P. H., Hansen, B., Siegel, D. I., Reeve, A. S., & Morin, P. J. (2004). Rates, pathways and drivers for peatland development in the hudson bay lowlands, northern ontario, canada. *Journal of Ecology*, *92*(6), 1036–1053.

Glaser, P. H., Siegel, D. I., Reeve, A. S., Janssens, J. A., & Janecky, D. R. (2004). Tectonic drivers for vegetation patterning and landscape evolution in the albany river region of the hudson bay lowlands. *Journal of Ecology*, *92*(6), 1054–1070.

Gorham, E. (1991). Northern peatlands: role in the carbon cycle and probable responses to climatic warming. *Ecological applications*, *1*(2), 182–195.

Guisan, A., Edwards Jr, T. C., & Hastie, T. (2002). Generalized linear and generalized additive models in studies of species distributions: setting the scene. *Ecological modelling*, *157*(2-3), 89–100.

Guo, M., Li, J., Sheng, C., Xu, J., & Wu, L. (2017). A review of wetland remote sensing. *Sensors*, *17*(4), 777.

Haapanen, R., & Tokola, T. (2007). Creating a digital treeless peatland map using satellite image interpretation. *Scandinavian Journal of Forest Research*, *22*(1), 48–59.

Herrera, L. P., Laterra, P., Maceira, N. O., Zelaya, K. D., & Martínez, G. A. (2009). Fragmentation status of tall-tussock grassland relics in the flooding pampa, argentina. *Rangeland Ecology & Management*, *62*(1), 73–82.

Hesse, R. (2010, 4). Lidar-derived local relief models âĂŞ a new tool for archaeological prospection. *Archaeological Prospection*, *17*(2), 67–72. Retrieved from http:https://doi.org/10.1002/arp.374 doi: 10.1002/arp.374

Houghton, J., Meira Filho, L., & Callender, B. (1995). *Climate change 1995: The science of climate change: contribution of working group i to the second assessment report of the intergovernmental panel on climate change* (Vol. 2). Cambridge University Press.

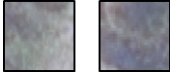Kéfi, S., Guttal, V., Brock, W. A., Carpenter, S. R., Ellison,

A. M., Livina, V. N., ... Dakos, V. (2014). Early warning signals of ecological transitions: methods for spatial patterns. *PloS one*, *9*(3), e92097.

Klinger, L. F. (1996). Coupling of soils and vegetation in peatland succession. *Arctic and Alpine Research*, 380–387.

Klinger, L. F., Elias, S. A., Behan-Pelletier, V. M., & Williams, N. E. (1990). The bog climax hypothesis: fossil arthropod and stratigraphic evidence in peat sections from southeast alaska, usa. *Ecography*, *13*(1), 72–80.

Klinger, L. F., & Short, S. K. (1996). Succession in the hudson bay lowland, northern ontario, canada. *Arctic and Alpine Research*, 172–183.

Kuhry, P., & Turunen, J. (2006). The postglacial development of boreal and subarctic peatlands. *Boreal peatland ecosystems*, 25–46.

Langanke, T., Burnett, C., & Lang, S. (2007). Assessing the mire conservation status of a raised bog site in salzburg using object-based monitoring and structural analysis. *Landscape and Urban Planning*, *79*(2), 160–169.

Lantäteriet. (2018). *Product description: Terrain map, vector (in swedish).* Retrieved from \url{https://www.lantmateriet.se/globalassets/kartor-och-geografisk-information/kartor/produktbeskrivningar/terrshmi.pdf}

Mathijssen, P. J., Kähkölä, N., Tuovinen, J.-P., Lohila, A., Minkkinen, K., Laurila, T., & Väliranta, M. (2017). Lateral expansion and carbon exchange of a boreal peatland in finland resulting in 7000 years of positive radiative forcing. *Journal of Geophysical Research: Biogeosciences*, *122*(3), 562–577.

McGarigal, K., Cushman, S. A., Neel, M. C., & Ene, E. (2002). *Fragstats: spatial pattern analysis program for categorical maps* (Tech. Rep.). United States Deparment of Agriculture.

Novák, D. (2014, 01). *Local relief model (lrm) toolbox for arcgis (update 2016-05 - new download link).*

Nungesser, M. K. (2011). Reading the landscape: temporal and spatial changes in a patterned peatland. *Wetlands ecology and management*, *19*(6), 475–493.

Ok, A. O., & Akyurek, Z. (2011). Automatic training site selection for agricultural crop classification: A case study on karacabey plain, turkey. *ISPRS Int. Arch. Photogramm. Remote Sens. Spatial Inf. Sci.*, *3819*, 221–225.

Poulin, M., Careau, D., Rochefort, L., & Desrochers, A. (2002). From satellite imagery to peatland vegetation diversity: how reliable are habitat maps? *Conservation ecology*, *6*(2), 16.

Påsse, T., & Daniels, J. (2015). *Past shore-level and sea-level displacements* (Report 137). SGU, Sveriges geologiska undersÃűkning. Retrieved from \url{http://resource.sgu.se/produkter/rm/rm137-rapport.pdf}

Rietkerk, M., Dekker, S., Wassen, M., Verkroost, A., & Bierkens, M. (2004). A putative mechanism for bog patterning. *The American Naturalist*, *163*(5), 699–708.

Rietkerk, M., Dekker, S. C., de Ruiter, P. C., & van de Koppel, J. (2004). Self-organized patchiness and catastrophic shifts in ecosystems. *Science*, *305*(5692), 1926–1929.

Scheffer, M., Bascompte, J., Brock, W. A., Brovkin, V., Carpenter, S. R., Dakos, V., ... Sugihara, G. (2009). Early-warning signals for critical transitions. *Nature*, *461*(7260), 53.

StatisticSweden. (2013). *Land use in sweden (markanvÃďndningen i sverige)* (Report). Statistics Sweden. Retrieved from \url{http://miljobarometern.malmo.se/content/docs/MI0803_2010A01B_BR_00_MI03BR1301.pdf}

Tuittila, E.-S., Juutinen, S., Frolking, S., VÃďliranta, M., Laine, A. M., Miettinen, A., ... MerilÃď, P. (2013). Wetland chronosequence as a model of peatland development: Vegetation succession, peat and carbon accumulation. *The Holocene*, *23*(1), 25-35. Retrieved from https://doi.org/10.1177/0959683612450197 doi: 10.1177/0959683612450197

Väliranta, M., Salojärvi, N., Vuorsalo, A., Juutinen, S., Korhola, A., Luoto, M., & Tuittila, E.-S. (2017). Holocene fen–bog transitions, current status in finland and future perspectives. *The Holocene*, *27*(5), 752–764.

Vitt, D. H., Bayley, S. E., & Jin, T.-L. (1995). Seasonal variation in water chemistry over a bog-rich fen gradient in continental western canada. *Canadian Journal of Fisheries and Aquatic Sciences*, *52*(3), 587–606.

Wieder, R. K., & Vitt, D. H. (2006). *Boreal peatland ecosystems* (Vol. 188). Springer Science & Business Media.

Wieder, R. K., Vitt, D. H., & Benscoter, B. W. (2006). Peatlands and the boreal forest. In *Boreal peatland ecosystems* (pp. 1–8). Springer.

Yu, Z., Campbell, I. D., Vitt, D. H., & Apps, M. J. (2001). Modelling long-term peatland dynamics. i. concepts, review, and proposed design. *Ecological Modelling*, *145*(2), 197–210.

A | Classification key

Table A.1 shows the amount of points used per class, per signature file (104 in total). In addition, it also gives examples of how each class can be recognised in a RGB image. The distinction between hummocks and hollows is the most difficult: they can both be similar in yellow colour. However the hummocks are often darker, and are more banded. Mudbottom is dark as well, however is well distinguishable from water. Sedge is the easiest to recognise, as it is the only green colour in peatlands (since forest is cut out).

Figure A.1 further shows where various spectral bands of classes overlap. Water is best distinguishable, followed by mudbottom. Hummocks and hollows show the most overlap.

Table A.1: *Classification key used in this study*

Class	# of points	Looks like
Hummock	30	
Hollow	30	
Mudbottom	20	
Water	9	
Sedge	15	

Class Name	Value	Color
Hummock	2	
Hollow	3	
Mud bottom	5	
Water	4	
Sedge	6	
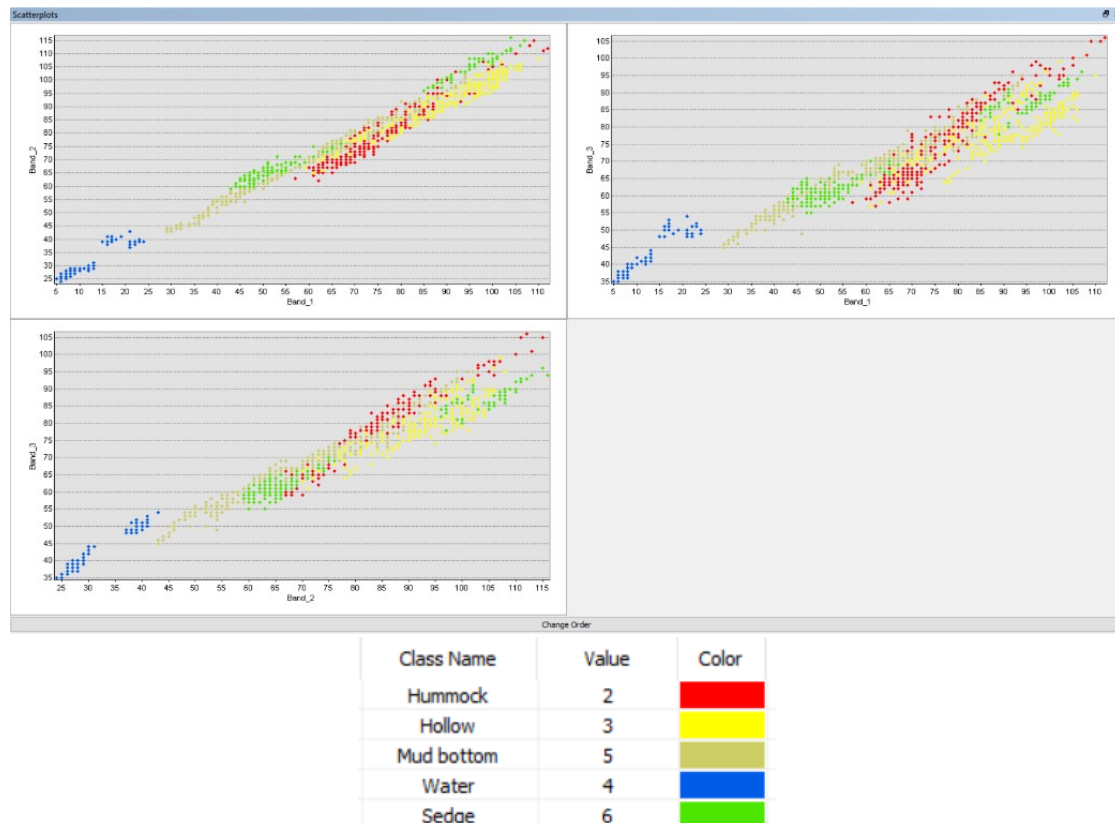
Figure A.1: *Scatterplot of spectral bands for the different classes*

B | Transect

Legend

Landcover
- Water
- Sedge
- Mud
- Hummock
- Hollow
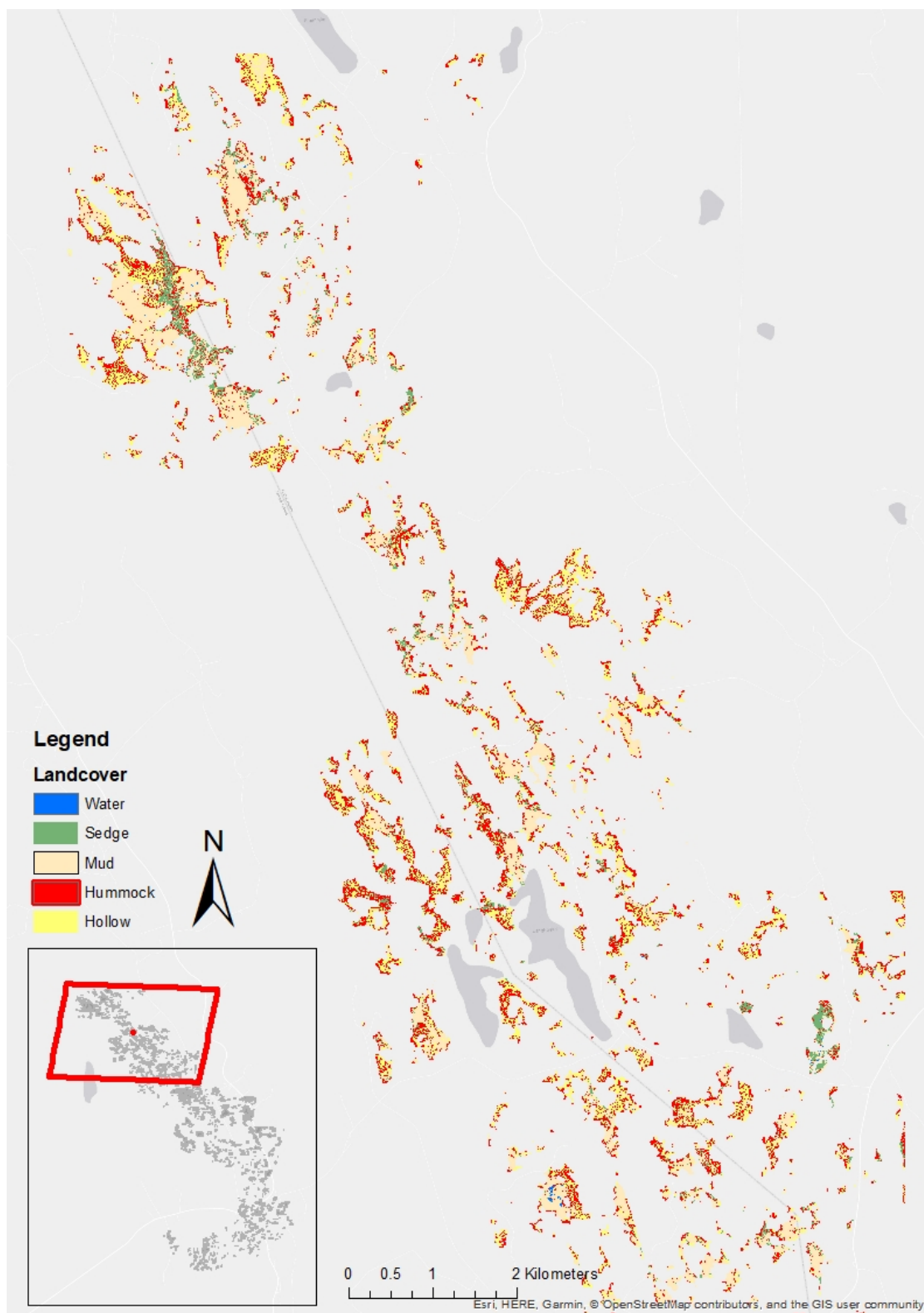
Figure B.1: Transect part 1

Legend

Landcover
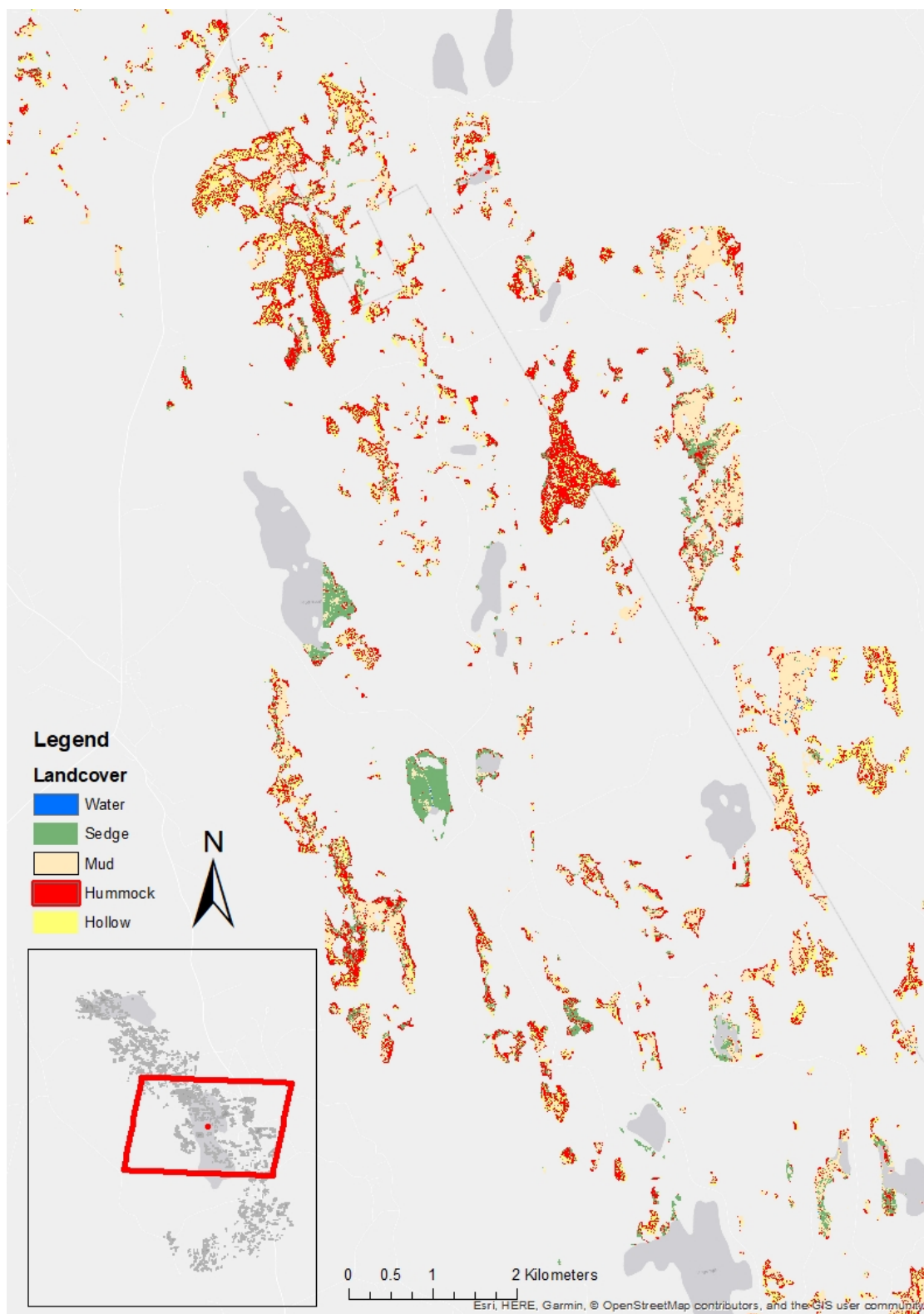- Water
- Sedge
- Mud
- Hummock
- Hollow

Figure B.2: Transect part 2

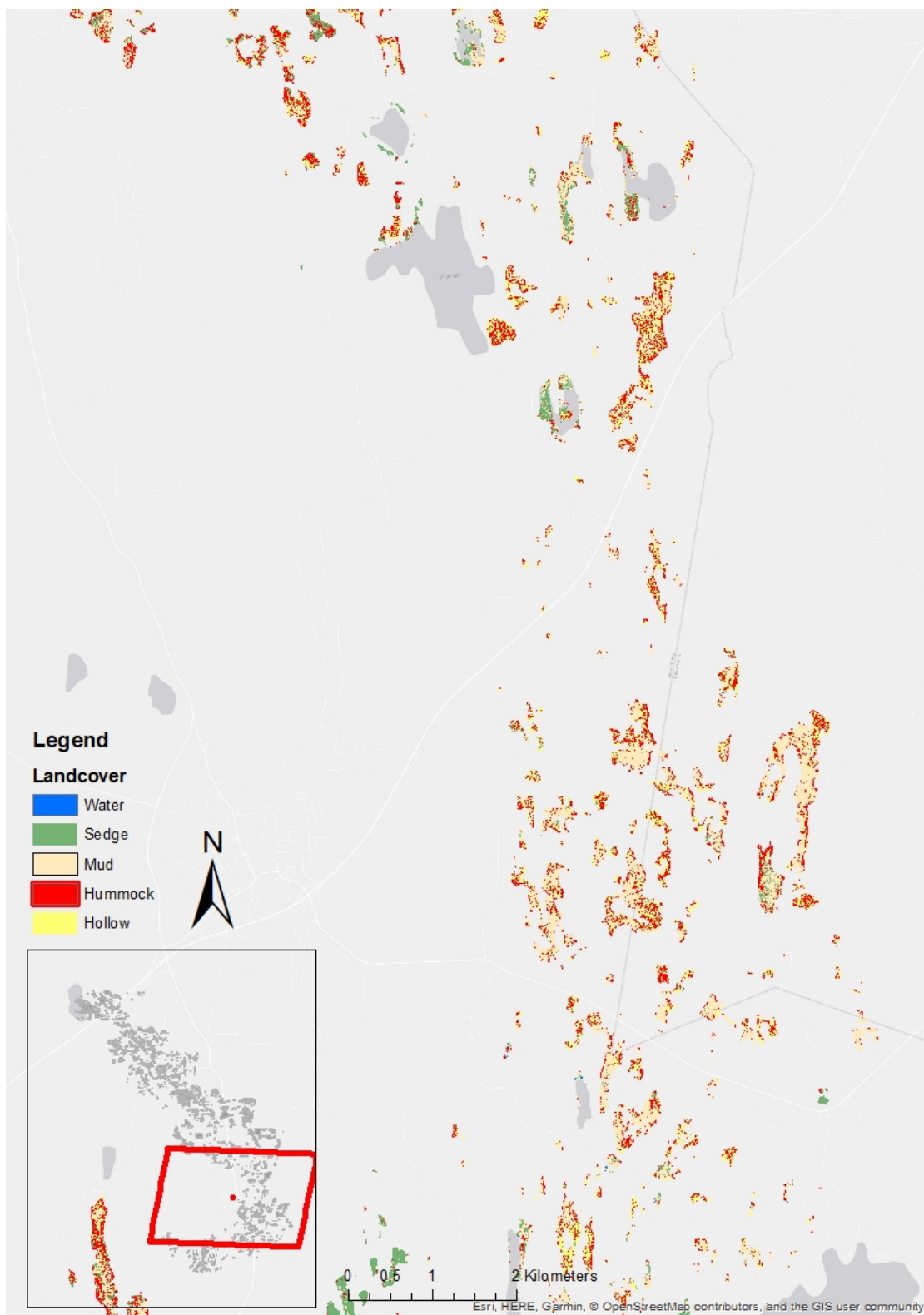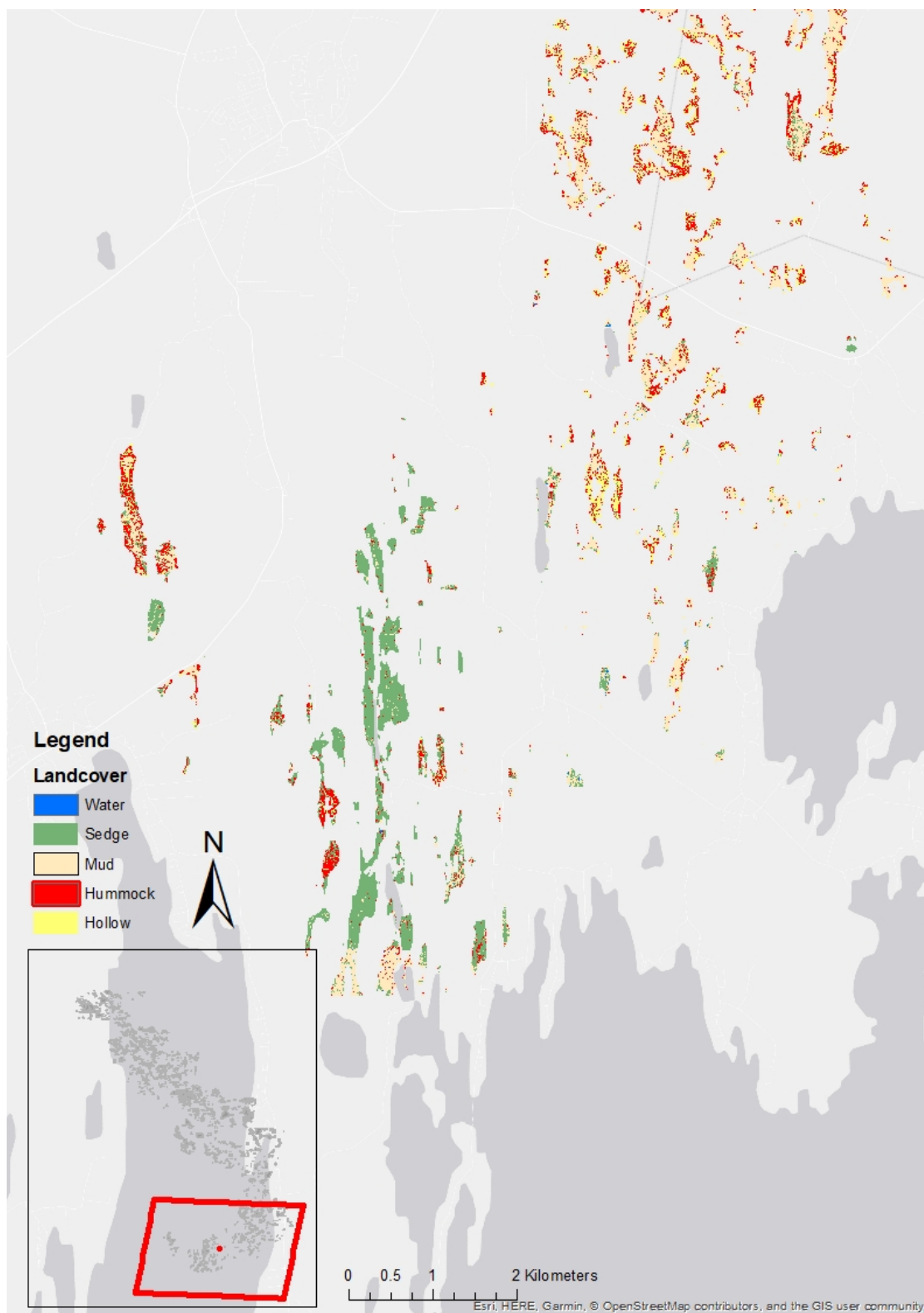**Figure B.3:** Transect part 3

Figure B.4: Transect divided into four parts
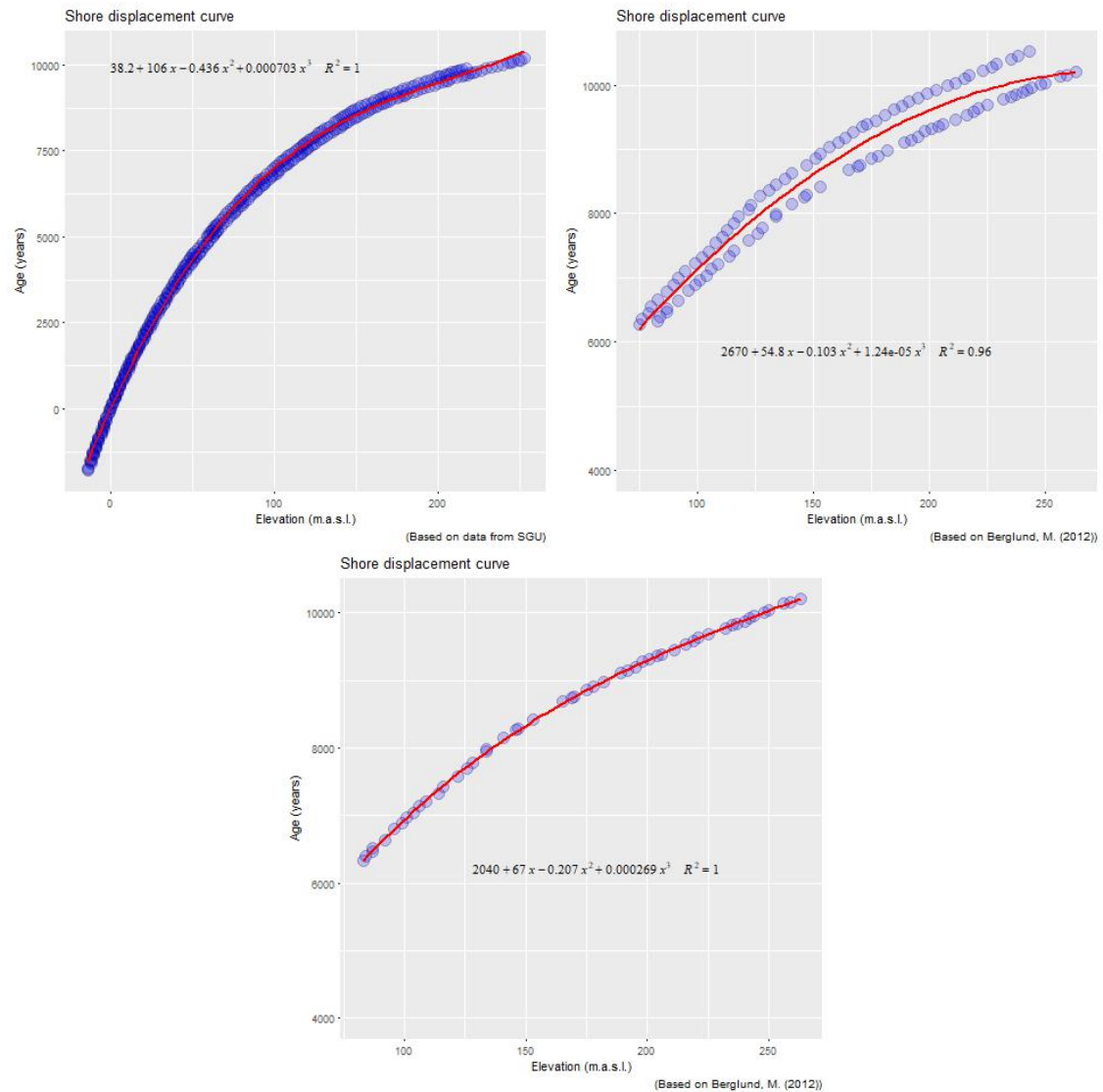
C | Shoreline displacement curves

Figure C.1: *Different shoreline displacement curves, from various sources*

Figure C.1 shows the different shoreline displacement curves, or age-elevation relationships, of various sources. A shows the curve from the Swedish geology website, 2 shows the curves from Berglund (2012) and 3 from Påsse and Daniels (2015)

D | Confusion matrix

Table D.1 shows the confusion matrix of the classification results using IR, G, B and a local DEM of 30m. 1= hummock, 2=hollow, 3=mudbottom, 4=water and 5=sedge. All classes were correctly classified, with Kappa = 1.

Table D.1: *Confusion matrix of classification, using IR, G, B and a local DEM of 30 m.*

		Reference				
		1	2	3	4	5
	1	5	0	0	0	0
	2	0	9	0	0	0
Prediction	3	0	0	2	0	0
	4	0	0	0	1	0
	5	0	0	0	0	4

E | Other age related metric GAM charts

Figure E.1 shows other age correlated metrics, namely: Contiguity Index (contig), Percentage of Like Adjacencies (pladj), area, number of patches (np), and Landscape Shape Index (lsi).
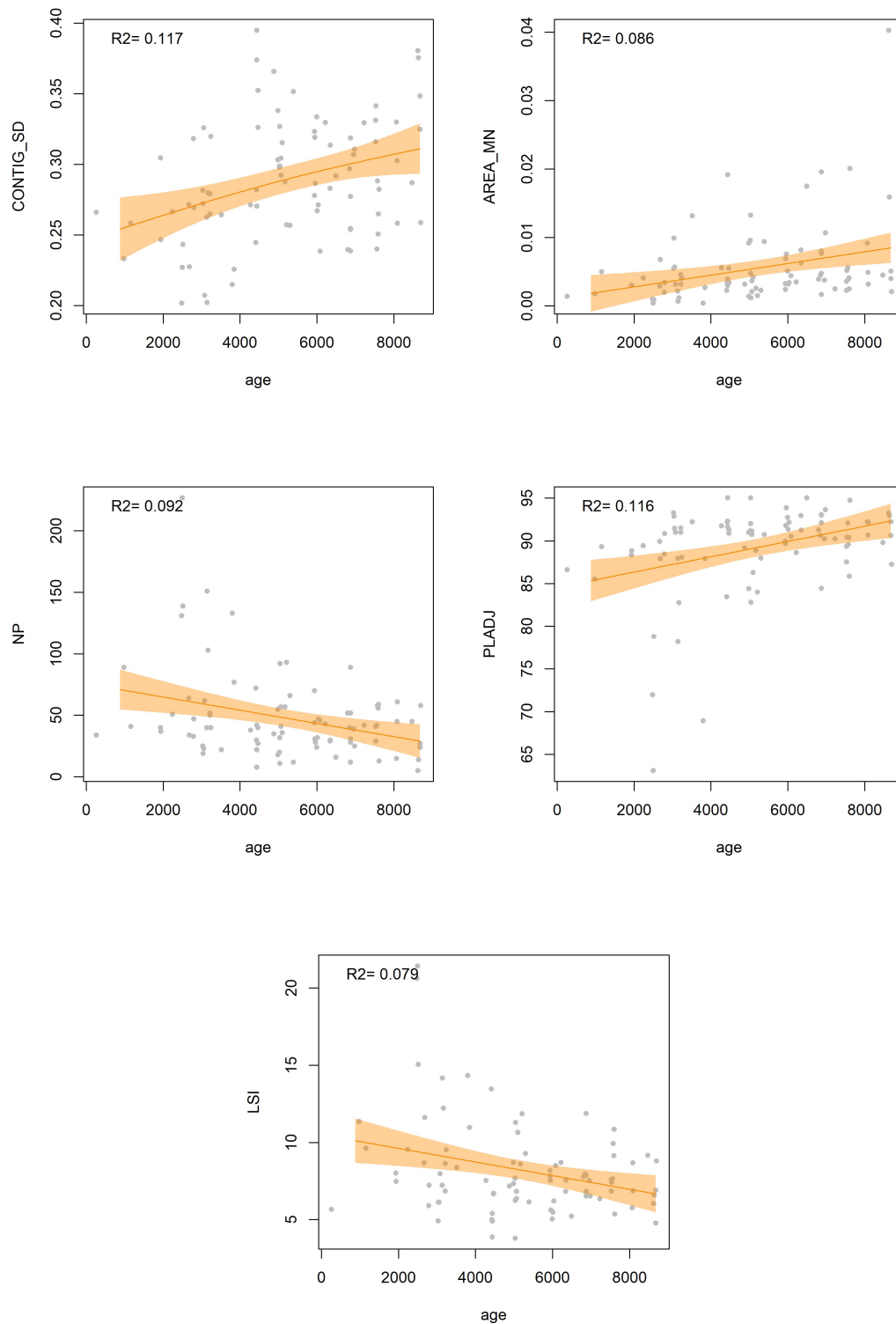

Figure E.1: *Different shoreline displacement curves, from various sources*

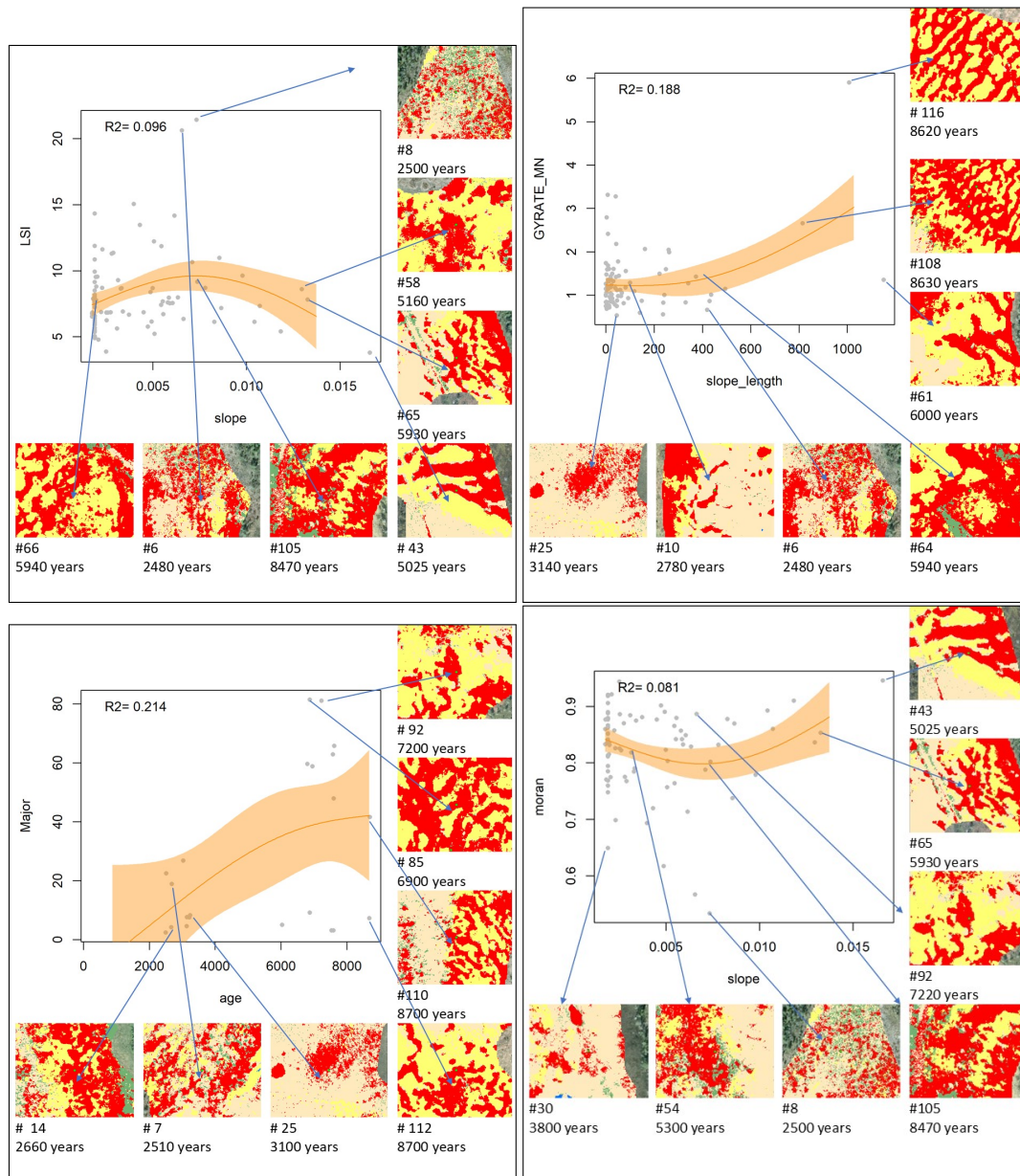# F | Terrain characteristic GAM figures

Figure F.1: GAM figures of different terrain characteristics

G | Correlation matrix

Figure G.1 shows a correlation matrix between all the terrain characteristics and pattern metrics. Blue means a high positive correlation, red means a high negative correlation.
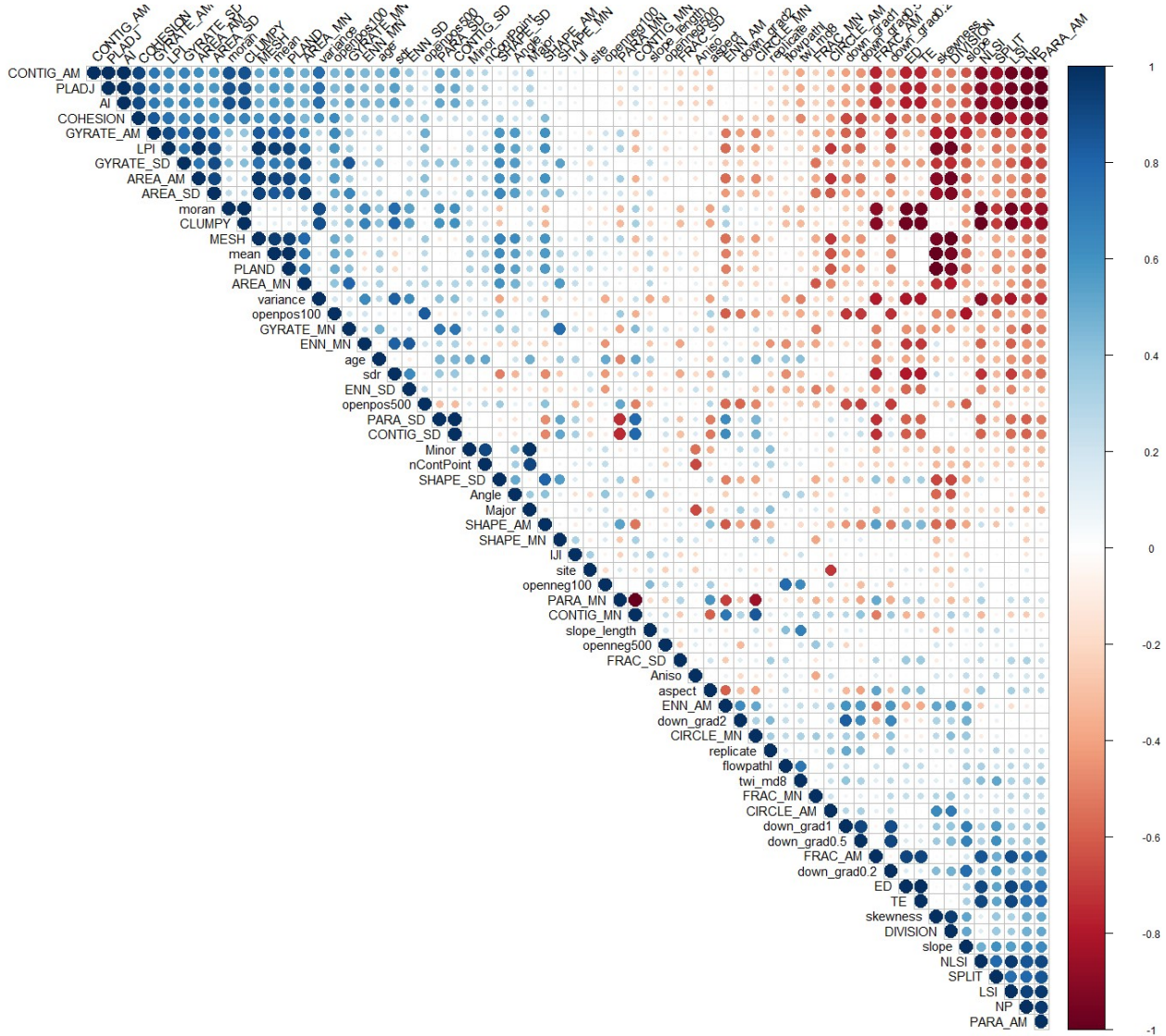

Figure G.1: *Correlation matrix of terrain characteristics and pattern metrics*